

## Response to Referee #1

Dear reviewer,

5 We all appreciate your hard work on this paper. These constructive opinions help to improve our work to a great extent. We did our best to respond to each comment and make this work well-organized. With the help of your detailed comments, some mistakes in the original manuscript were found and revised. Details are listed as follows:

Major comments:

10 (1) There are substantial differences between the CS and TS in TKE,  $u^*$ , and even W and U (Fig. 2). One can use these quantities in the explanation of accumulation and diffusion of PM<sub>2.5</sub>. Why do we need an IF index? In other words, what is the advantage or superiority of using IF compared with other quantities? This point should be discussed in the paper.

15 **Response:** Thank you for your comments. In previous works, some traditional variables (i.e. TKE,  $u^*$ , and W/U) are commonly applied to indicate the behavior of turbulence. And the results in our work (Fig. 2) also show the relationship between those variables and the accumulation and diffusion of PM<sub>2.5</sub> to some extent. Indeed, those quantities are useful for the description of turbulent characteristics including strength and variation, but fail to reveal the intermittency of turbulence. As mentioned in the introduction, the reason why we focus mainly on the influence of intermittent turbulence is that the intermittent turbulence accounts for a large amount of vertical fluxes in stable boundary layers but the discussion of the effects of intermittent turbulence on the transport of PM<sub>2.5</sub> is still limited. At this point, we need an effective way to describe the characteristics of turbulent intermittency.

20 The IF index was developed from the arbitrary-order Hilbert spectral analysis (arbitrary-order HSA, Huang et al., 2008). Compared with some classic methods (such as Fourier analysis and wavelet transform), the arbitrary-order HSA technique is intuitive, direct, and adaptive, with a posteriori-defined basis, from the decomposition method, based on and derived from the data, it is more appropriate for the analysis of nonlinear and non-stationary turbulence signals. Our some previous work (Wei et al. 2017) has addressed the intermittency of turbulence in the SBL using the arbitrary-order HSA technique. But we should admit that, as a newly-developed approach, arbitrary-order HSA still suffers some disadvantages. For example, the spline fitting and the end effects need more improvements. In the case of weak signals imbedded in stronger ones, differentiation should be applied if needed. In spite of these problems, HSA is still the best available nonlinear and non-stationary data analysis method so far.

25 Based these considerations, we used the arbitrary-order HSA in this work to study the behavior of turbulent intermittency. The advantages of IF or arbitrary-order HSA are addressed in the revision according to your advice: “Based on the arbitrary-order HSA, we proposed an index, called intermittency factor (IF), to quantify the level of turbulent intermittency, which is assumingly more effective compare with some classic quantities.” (page 5 lines 10-13) and “As one of the most important steps through this method, the empirical mode decomposition separates the original time series into different modes based on its own physical characteristics without any predetermined basis, implying an intuitive, direct, adaptive, and data-based nature” (page 6 lines 22-24). Some

more detailed information is given in the supplement:

“The reason why the arbitrary-order HSA is applied to this work is that this method is more suitable for the analyses of nonlinear and non-stationary turbulent signals, compared with traditional techniques, such as Fourier analysis and Wavelet transform. It is known that, the data, whether from physical measurements or numerical modeling, most likely will have some problems: (a) the total data span is too short; (b) the data are non-stationary; and (c) the data represent nonlinear processes. While the Fourier analysis has some crucial restrictions: the system should be linear; and the data should be strictly periodic or stationary; otherwise, the resulting spectrum will make little physical sense. However, for lack of alternatives, Fourier spectral analysis is still applied to many kinds of data which may result in misleading results. On the other hand, the wavelet approach is essentially an adjustable window Fourier spectral analysis, with the basic wavelet function that satisfies certain very general conditions. As the traditional technique for the analysis of intermittency, the structure function is essentially associated with the Fourier decomposition, which means that the scaling exponent function  $\zeta(q)$  has some limitations in the application of nonlinear and non-stationary turbulence signals.” (page 4 lines 9-21 in the supplement)

“As discussed by Huang et al. (1998, 1999), the arbitrary-order HSA technique is intuitive, direct, and adaptive, with a posteriori-defined basis, from the decomposition method, based on and derived from the data, it is more appropriate for the analysis of nonlinear and non-stationary turbulence signals. Since its introduction, the HSA method has been successfully applied into different fields, including climatology (Molla et al. 2006; Hu et al. 2014), meteorology (Karipot et al. 2009; Vincent et al. 2011) and oceanography (Chen et al. 2014), to name just a few. One of the authors (Wei et al. 2017) used arbitrary-order HSA technique to separate fine-scale and large-scale motions in the stable boundary layer (SBL) and obtained a better approximation to the Monin-Obukhov similarity theory than using bandpass filtering method. Based on these considerations and previous work, we believe that the arbitrary-order HSA technique is a suitable method for the study of turbulence intermittency in the SBL.” (page 4 line 21 and page 5 lines 1-9 in the supplement)

(2) Are there any significant correlations between IF and TKE as well as other parameters? If there are, they should be presented and discussed.

**Response:** Thank you for your suggestion. We examined the relationship between IF and other quantities, including  $u^*$  as the dynamic parameter and  $z/L$  as the thermodynamic variable, and the results are shown as follows:

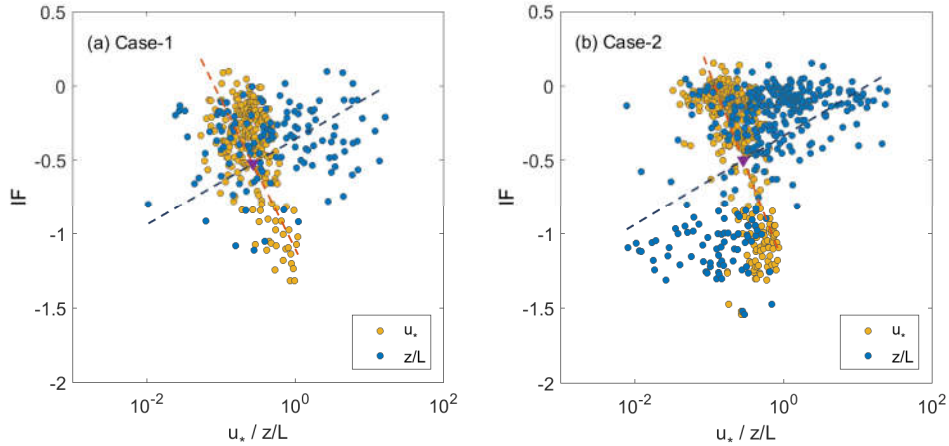


**Figure 1** Scatter plot comparing IF and other variables ( $u_*$  and nighttime  $z/L$ ) for two cases at 40 m. The dashed lines are the fittings from least-squares regression and the triangle marks the cross point.

5

Generally, the values of IF decrease with increasingly stronger turbulence, which meets our expectation. Under extremely strong stable conditions, the turbulence in the ABL is suppressed, accompanied by very small dynamic quantities (such as  $u_*$  in this case). At this point, the values of IF are nearly zero, representing the extremely weak turbulent fluctuation. With the increase of turbulence strength, the abstract value of IF rises, indicating that the relatively stronger turbulence in the ABL is intermittent but not continuous or fully-developed. In order to confirm these conclusions, the distribution of IF with stability function  $z/L$  during the nighttime is given in Figure 1 as well. Under strong stable conditions (i.e.  $z/L \gg 1$ ), turbulence is weak and IF is nearly zero. While the weak stable cases (i.e.  $z/L \approx 0.1$ ) are accompanied by active turbulence but larger negative IF.

10

15

This part is added to the revision as in: “Fig. 7 further confirms the relationship between IF and  $u_*$  or  $z/L$ , in which dots of strong turbulence ( $u_*$ ) and weak stable stratification ( $z/L \approx 0.1$ ) mainly come from the TS. Larger deviation of IF occurs accompanied by increasing turbulent strength when stability in the ABL becomes weaker. That is, intermittent turbulence (marked by large negative values of IF) leads to strong fluxes during the TS.” (page 13 lines 7-10) and Fig.7 (page 14).

20

(3) Your measurements are from Tianjin, which is just west of the Bohai Bay. The emission and formation of PM<sub>2.5</sub> over the land areas are much stronger than over the sea. Therefore, I guess air from the Bohai Bay was much cleaner. During each TS the prevailing wind was either southeasterly or northeasterly, different from that during the CSs. Did the change in horizontal air flow contribute also to the decrease in the PM<sub>2.5</sub> concentration? And how significant?

25

**Response:** We really appreciate your constructive questions. Firstly, we must apologize that there is

something wrong with the wind vector in Fig. 2. We have carefully checked through the raw data and corrected the drawing program. The right wind vector at three levels (40, 120, and 200 m) for two cases is shown in the following Figure 2 and Figure 3 is the corresponding rose diagram of wind direction. From the results of Figure 2, the CS is characterized by south-easterly wind. When it comes to the TS, the wind predominately originates from west or north-west. Although the wind vector of Case-2 in Figure 2 is relatively disordered, the rose diagram in Figure 3 reveals that the most common wind direction for the CS ranges from east to south-east and the flow during the TS is mainly from the west, which is consist with the results of Case-1. Previous works have given plenty of solid evidence on the impacts of local and synoptic circulation on the accumulation and transport of air pollutants in the North China Plain. Considering that the main purpose of this work focuses on the vertical transport by turbulent mixing, we just cited some recently published paper (including Zhang et al., 2017; Miao et al., 2017; Ye et al., 2016; Zhang et al., 2012; Zheng et al., 2015a; Jiang et al., 2015) in the introduction (see page 2 line 4). Here we try to address it in detail. Tianjin is surrounded by Hebei province and also located to the north of western Shandong and northern Henan province, which are the most densely pullulated regions with the fastest growing economy in Northern China recently (Wang et al., 2014). In this case, the contribution to the PM concentration by cross-city transport from neighboring province cannot be neglected. Using modeling study, Jiang et al. (2015) revealed that the southerly wind at lower layer contributes to transport PM from the southern neighboring cities with serious pollution. Furthermore, air masses from the south are warmer and wetter than the northern air masses, thus possessing a higher specific humidity, which facilitates the secondary formation by heterogeneous reactions (Zheng et al., 2015a). In terms of transport stage, Zheng et al., (2015a) found that weather pattern for the clean hours are normally characterized by strong high-pressure centers northwest of the polluted region in winter (i.e., the Siberian anticyclone), resulting in strong north-westerly wind.

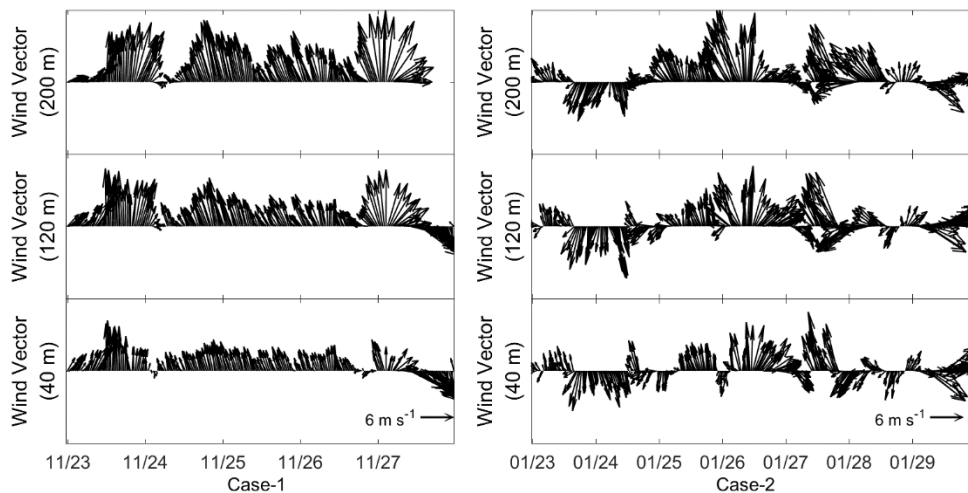
We are also thankful for your revealing comment on the sea breeze. It is reasonable to expect that the flows from the Bohai sea would be helpful to improve the air quality in Tianjin, but the work by Miao et al. (2015) provides an opposite conclusion. Their modeling results show that the southerly ambient wind brings lots of aerosols emitted from southern region to the Bohai sea and then sea breeze transports marine air together with the aerosols to the land.

All of these works above present the importance of horizontal circulation in the transport of  $PM_{2.5}$ . However, some works (Zheng et al., 2015a; Chan and Yao, 2008) mentioned that in the case of city clusters, air pollution may not be eliminated solely by advection. This is because the pollution is formed in the city cluster, there is no clean air from upwind, resulting in more persistent pollution events. There is no doubt that horizontal transport is crucial to the decrease in the  $PM_{2.5}$  concentration, but the mechanisms of polluted events are complicated and we try to explore the effect of intermittent turbulence from a new angle.

We are so sorry for the errors in the wind vector in Fig. 2 and they have been corrected in the revision. Besides, in order to enrich this work, some previous results on the local circulation are introduced in page 7 lines 14-22:

“For Case-1, wind at lower levels mainly comes from the south-east during the CS, while the dominant wind direction turns into west when it comes to the TS. Although the wind direction for Case-2 is seemingly unsteady in Fig. 2, the statistical the rose diagrams (see Figure S8) confirm a

5 similar result, with south-easterly flows dominating the CS and westers for the TS. This wind-direction pattern is in agreement with previous works (Zhang et al., 2017; Miao et al., 2017; Zheng et al., 2015a; Jiang et al., 2015). They found that south-easterly wind can bring the aerosols emitted by the surrounding cities to this region while the clean hours is normally characterized by strong high-pressure centers northwest of the polluted region in winter. However, in the region with densely distributed mega-cities (as in the case of Tianjin), because the upwind flows is polluted, mere advection may not be enough to disperse pollutants, thus resulting in persistent air pollution events (Zheng et al., 2015a; Chan and Yao, 2008).”



10 **Figure 2** Wind vector at three levels. The left panel is for Case-1 and the right panel is for Case-2.

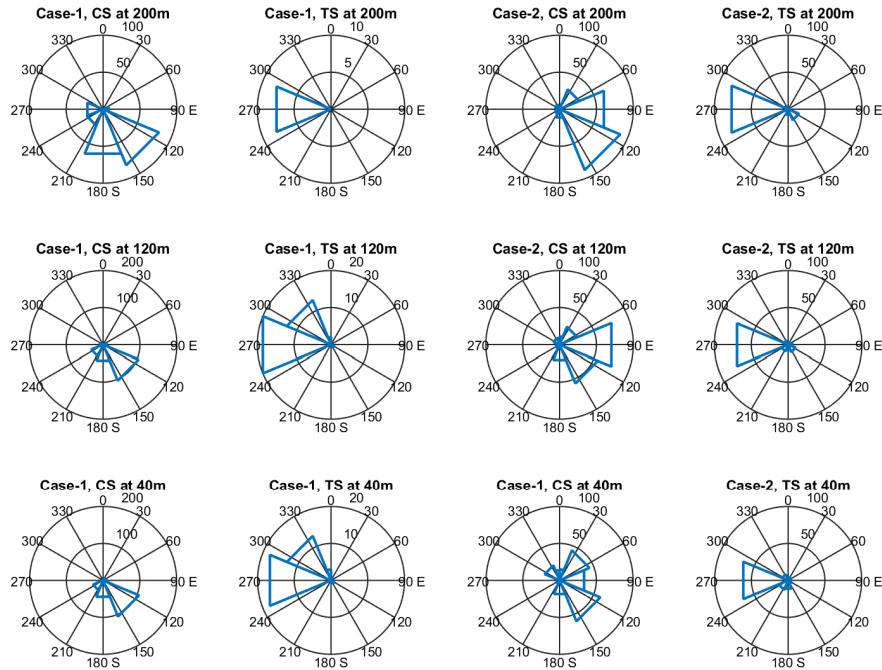


**Figure 3** Comparison of rose diagram between the CS and the TS for two cases at three levels.

(4) You show in Fig. 3 vertical profiles of changes in potential temperature during the CSs. I think similar results for the TSs should be presented and discussed as well. You may show how rapidly the stable condition formed during the CSs was broken by intermittent turbulence. In addition, some discussions about the evolution of the PBL height may be also good for a more complete picture.

**Response:** Thank you so much for your constructive advice. The change in potential temperature during the CS and the TS is both presented in Fig.3 (a–f) in the reversion. Compared with the clear warming at high levels during CSs, the high-level cooling during TSs is significant (see Fig. 3 d–f), implying the collapse of inversion layer when it comes to the TS. Meanwhile, Fig. 3g gives the daily mean potential temperature profiles from 23 to 28 November to illustrate the evolution of inversion layer. We can see that the inversion layer gradually developed from 23 to 27 November but rapidly collapsed on 28 November. Since there is no radio soundings available near Tianjin site, we simulated the Planetary Boundary Layer Height using WRF model. The model configuration can refer to the work by Zheng et al. (2015c) which focused on a haze event in 2013 of this region. Details are given as follows:

“Fig. 3 depicts the distribution of Planetary Boundary Layer Height (PBLH) and the daily mean potential temperature profiles at 15 different heights, including change of  $\theta$  over the CS (Fig. 3a–c) / TS (Fig. 3d–f) and the development during the whole polluted event (Fig. 3g). The  $\Delta\theta$  at given height of CSs was calculated by subtracting the value of  $\theta$  on the last day from that on the first day.

And so it does for TSs. For Case-1,  $\Delta\theta$  during the CS at the lowest level (5 m) is only 5.2 K. But for the top level at 250 m,  $\Delta\theta$  is relatively larger with a value of 6.8 K. This result confirms that the warming of upper layers is stronger than that of lower layers, implying an increasingly stably stratified boundary layer during polluted days. Figs. 3b and 3c for Case-2 verify this conclusion as well. On the contrary,  $\Delta\theta$  during TSs (Fig. 3d–f) presents a significant cooling at higher levels, denoting the collapse of inversion layer at the end of the polluted event. Taking Case-1 as an example, Fig. 3g depicts the evolution of inversion layer. It can be seen that the inversion layer was gradually enhanced from 23 to 27 November but quickly depressed on 28 November, which verifies the results of Fig. 3a–f. Fig. 3h illustrates the distribution of PBLH, which is simulated with the Weather Research & Forecasting (WRF) Model (Zheng et al., 2015c). In Fig. 3h, the PBLH for Case-1 gradually decreased and reached its minimum on the night of 26–27 November. Then the PBLH redeveloped to higher than 1,300 m during the daytime of 28 November.” (page 7 lines 29-33 and page 8 lines 1-9)

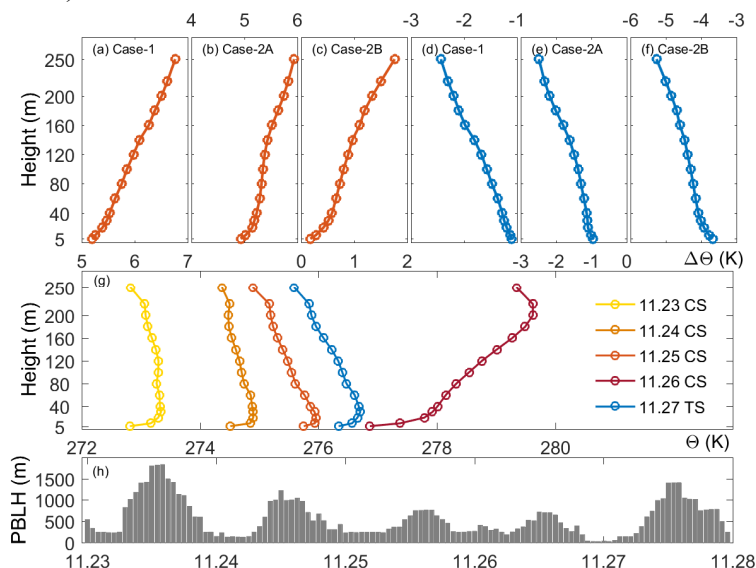


**Figure 4** Vertical distribution of daily mean potential temperature. The change of daily mean potential temperature of CSs is showed in (a)–(c) and (d)–(f) are for TSs. (g) illustrates the evolution of inversion layer of Case-1. (h) is the PBLH simulated with WRF Model.

(5) Your results and conclusions are based on cases study. I think it is better to add “cases from Tianjin” or similar subtitle. And “vertical diffusion” in the title can be questionable if you cannot prove that the decrease in PM<sub>2.5</sub> was solely due to the vertical diffusion.

**Response:** Thank you for your suggestion. We specified “cases from Tianjin” in the revision. But considering that there have been a lot of work aiming on the horizontal transport of PM<sub>2.5</sub>, we mainly focus on the effect of vertical mixing of intermittent turbulence. Indeed, the reasons for the transport of particles are complicated, including climate change, synoptic circulation, and boundary layer structures and we cannot address them all. So far, there is limited works on the intermittent



turbulence under strongly stable conditions. Therefore, we keep “vertical” in the new title to emphasize the effects of vertical turbulent mixing and we hope you will approve of our modification. The new title is “Intermittent turbulence contributes to vertical dispersion of PM<sub>2.5</sub> in the North China Plain: cases from Tianjin”.

5

Minor points:

Page 1 line 21: What do you mean by “wind filed”? Wind profile?

**Response:** Yes, it should be “wind profile” and has been rewritten.

10 Page 2 line 21: Define “FI”.

**Response:** “FI” is defined as flux intermittency by Mahrt (1998).  $FI = \sigma_F / \text{abs}[F]$ , in which  $\sigma_F$  is the standard deviation of the 5-minute averaged flux and  $\text{abs}[F]$  is the absolute value of the one-hour average of the flux.

15 The manuscript has been corrected as well. “FI index (Flux Intermittency, Eq. (9) in Mahrt, 1998)” (page 2, lines 21-22)

Page 2 line 32: Delete “respectively”.

**Response:** Yes.

20 Page 3 line 4: Change “east” to “southeast”.

**Response:** Yes.

Page 3 line 11: I think “HMP45C” is the type name of the probe and should be put in the brackets.

**Response:** This has been corrected.

25

Page 3 line 16: Was the TEOM system installed near the tower or the WPR? Please make it clear.

**Response:** Thank you for your question. The TEOM system used in this study is mounted near the 255-m tower. The distance between the 255-m tower and the TEOM system is around 2.3 km. The location of the TEOM system is specified as follows:

30 “The 1405-DF TEOM system is located nearly 2.3 km away from the 255-m tower to the east and installed at a height of 3 m to monitor the surface PM<sub>2.5</sub>.” (page 3 lines 15-17)

Table 1: “c: 300-366 m s<sup>-1</sup>”. Is this the range of wind speed that the sonic anemometer can measure? 300 is a very strange number here.

35 **Response:** Here c represents the speed of sound which is used to calculate the sonic virtual temperature. According to the instruction manual of CSAT3 Three Dimensional Sonic Anemometer, the range of speed of sound is from 300 to 366 m s<sup>-1</sup> (–50 to +60 °C). The definition of c is added to Table 1.

Page 4 line 16: Change “poor data” to “poor quality of data”.

40 **Response:** Yes, thank you.

Page 4 lines 19-21: What are the criteria for data that are suitable for this study?



**Response:** All of the data used in this study were checked strictly. The quality control for turbulence observations includes error flag, spike detection, cross wind correction, spectral loss correction, sonic virtual temperature correction, density fluctuation correction, and coordinate rotation. “If more than 20% points within a given 30-min time series were detected as outliers, then this 30-min observation was discarded.” (page 4 lines 10-11) The wind profiles were checked time by time. “First, data below 200 m were removed due to the interference of surrounding environment, including trees and buildings. Then each vertical profile was checked through and points with larger than 2.5 standard deviations were regarded as outliers and discarded. (page 4 lines 17-19)” And according to previous study in this region (Wei et al., 2014), a profile was discarded if more than 40% of the data points were outliers or missing.

Page 5 line 2: “local standard time” or “Beijing Time”?

**Response:** Yes, it should be “Beijing Time”.

Page 5 line 9: “On this basis”? It is not clear what is denoted.

**Response:** We mean that based on the arbitrary-order HSA, we developed IF. This has been corrected.

Page 5 lines 11-12: Delete “(CSAT3, CAMPBELL Inc., USA)” because the same information is given on page 3.

**Response:** It has been deleted.

Page 5 line 19: Do you mean the local maxima that are found within every 30-min periods?

**Response:** Yes, here the local maxima are from the 30-min time series  $X(t)$ . This has been corrected as:

“The first step is to form the upper envelope  $e_{max}(t)$  based on the local maxima of 30-min  $X(t)$ ” (page 5 lines 21).

Page 5 line 9, page 6 lines 12-13, and page 11 lines 18-19: You are proposing or defining IF at these three places. This is redundant. I think you should define the IF index at a suitable place and use it elsewhere.

**Response:** Thank you for pointing out that. The IF index is defined when it is first mentioned (page 5 line 11) and other definitions have been deleted.

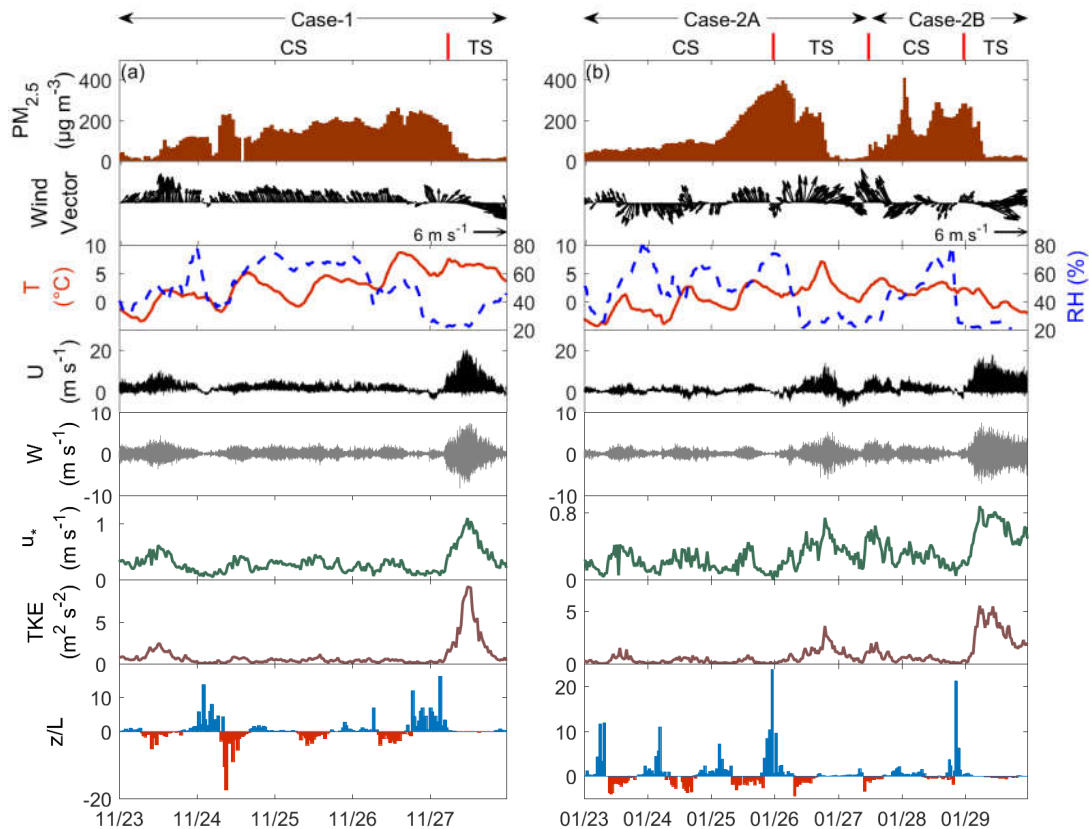
Page 6 line 31 and page 7 line 1: “. . . increased to a maximum of 412  $\mu\text{g m}^{-3}$  for PM<sub>2.5</sub> and then dropped to a low level within a few hours no matter for Case-1 and Case-2”. Please check your expression. I do believe the maximum values in Fig. 2a and Fig. 2b are all 412.

**Response:** Thank you for your question. The maximum for Case-1 is 263  $\mu\text{g m}^{-3}$  and 412  $\mu\text{g m}^{-3}$  for Case-2. This part has been rewritten in the revision.

“it can be seen that the concentration of PM<sub>2.5</sub> gradually increased to maxima (263  $\mu\text{g m}^{-3}$  for Case-1 and 412  $\mu\text{g m}^{-3}$  for Case-2) and then dropped to a low level within a few hours.” (page 7 lines 5-6)

Page 9 Fig. 2: Please add some ticks on the Y-axes of Figs. 2a and 2b.

**Response:** The Fig. 2a and 2b have been replotted with ticks.



Page 11 line 2: CSs or TSs?

**Response:** We are sorry for the slip of the pen. It should be “TSs”.

5

Page 11 Fig. 5: Does each concave curve represent a 30-min result? Please make it clear.

**Response:** Yes, each curve in Fig. 5 is from a 30-min vertical wind speed signal, which has been clarified in the caption of Fig. 5.

10 “Hilbert-based scaling exponent function at 40 m during different stages for (a) – (b) Case-1 and (c) – (d) Case-2, where each dashed curve represents the result of 30-min vertical wind speed signal and the black solid line denotes the K41 result  $q/3$ .” (page 12 and lines 15-16)

Page 11 line 24: Delete “site”.

**Response:** Yes.

15

Page 13 line 2: “under stable conditions”? Are you not talking about the TS?

**Response:** Thank you for your question. We have replaced “under stable conditions” with “in the ABL”.

20

## References

- Huang, Y. X., Schmitt, F. G., Lu, Z. M., & Liu, Y. L. (2008). An amplitude-frequency study of turbulent scaling intermittency using empirical mode decomposition and Hilbert spectral analysis. *EPL (Europhysics Letters)*, 84(4), 40010.
- 5 Wei, W., Zhang, H. S., Schmitt, F. G., Huang, Y. X., Cai, X. H., Song, Y., ... & Zhang, H. (2017). Investigation of Turbulence behaviour in the stable boundary layer using arbitrary-order Hilbert spectra. *Boundary-Layer Meteorology*, 163(2), 311-326.
- Chan, C. K., & Yao, X. (2008). Air pollution in mega cities in China. *Atmospheric environment*, 42(1), 1-42.
- 10 Jiang, C., Wang, H., Zhao, T., Li, T., & Che, H. (2015). Modeling study of PM 2.5 pollutant transport across cities in China's Jing-Jin-Ji region during a severe haze episode in December 2013. *Atmospheric Chemistry and Physics*, 15(10), 5803-5814.
- Miao, Y., Guo, J., Liu, S., Liu, H., Zhang, G., Yan, Y., & He, J. (2017). Relay transport of aerosols to Beijing-Tianjin-Hebei region by multi-scale atmospheric circulations. *Atmospheric*
- 15 *Environment*, 165, 35-45.
- Wang, H., Tan, S. C., Wang, Y., Jiang, C., Shi, G. Y., Zhang, M. X., & Che, H. Z. (2014). A multisource observation study of the severe prolonged regional haze episode over eastern China in January 2013. *Atmospheric Environment*, 89, 807-815.
- Wei, W., Zhang, H. S., & Ye, X. X. (2014). Comparison of low - level jets along the north coast of
- 20 China in summer. *Journal of Geophysical Research: Atmospheres*, 119(16), 9692-9706.
- Zheng, G. J., Duan, F. K., Su, H., Ma, Y. L., Cheng, Y., Zheng, B., ... & Pöschl, U. (2015a). Exploring the severe winter haze in Beijing: the impact of synoptic weather, regional transport and heterogeneous reactions. *Atmospheric Chemistry and Physics*, 15(6), 2969-2983.
- Zheng, B., Zhang, Q., Zhang, Y., He, K. B., Wang, K., Zheng, G. J., ... & Kimoto, T. (2015c).
- 25 Heterogeneous chemistry: a mechanism missing in current models to explain secondary inorganic aerosol formation during the January 2013 haze episode in North China. *Atmospheric Chemistry and Physics*, 15(4), 2031.

## Response to Referee #2

Dear reviewer,

5 Thank you so much for all these recommendations. The manuscript has been refined following your advice. In order to enrich this work, some more detailed information on the methodology is given in a supplement due to space limit. The detailed responses are as follows:

10 This manuscript investigates the role of intermittent turbulence in alleviating heavy pollution episodes that frequently occur in China. The papers includes a theoretical background and analysis of measurement data related to 2 pollution episodes. While the vast majority of the prior research on air pollution episodes in China has concentrated on the factors favoring the accumulation of pollutants, this paper investigates a phenomenon that helps to get rid of high pollution levels. As such, I think that this paper is original enough to warrant publication in ACP. I have a few issues that should, however, be  
15 addressed before the publication.

The authors introduce an Intermittent Factor (IF) which they use for explaining the effects of intermittent turbulence on the observations. I have a few comments on this. First, it seems that  $q$  is the key variable when determining IF. Therefore, the authors should explain more explicitly what is the exact meaning of  $q$ , not just to mention that it is the power exponent of the instantaneous amplitude of something. Second, IF is defined such that it is zero for fully developed turbulence and negative if not. However, the exact value of IF does not tell anything for the reader. Would it be possible to provide some idea how to interpret the value of IF. How small (or large in absolute sense) should IF be for the intermittent turbulence to be important etc?

25 **Response:** We all appreciate your constructive comments. A sketch of the arbitrary-order HSA has been given in the manuscript, including the derivative process, equations and a brief comparison with existing methods, (i.e., Fourier analysis and wavelet transform). Due to lack of space, we cannot address the method and the relative parameters fully in the manuscript, so we write a supplement (Figure S1-S6 and the relative illustration) to describe the process of the arbitrary-order HSA.

30 As you pointed out,  $q$  is an important parameter in the derivation of scaling exponent function  $\xi(q)$  for several reasons. Firstly,  $q$  is the moment of the arbitrary-order Hilbert spectrum  $\mathcal{L}_q(\omega) = \int p(\omega, A)A^q dA$ . If  $q$  is taken as 2, the second-order Hilbert spectrum  $\mathcal{L}_2(\omega) = \int p(\omega, A)A^2 dA$  can be an analogical representation of classic Fourier energy spectrum, given that the square of amplitude is equivalent to energy density. Secondly, in the identification of the range of scale invariance, the third-order Hilbert spectrum  $\mathcal{L}_3(\omega) = \int p(\omega, A)A^3 dA$  is taken as the reference. Kolmogorov's initial proposal leads to  $\zeta(q) = q/3$  (Kolmogorov, 1941), while the scaling exponent function  $\zeta(q)$  of intermittent turbulence is nonlinear and concave. Only  $\zeta(3)$  has no intermittency correction, that is,  $\zeta(3) = 1$ . Finally, the highest moment of  $\zeta(q)$  considers both  
35 computing efficiency and accuracy in the measurements of high-order moments. The higher the order is, the longer the length of sample needs, while the arbitrary-order HSA process of long data will take a lot of time. Therefore, the maximal moment is taken as  $q_{max} = 4$ . The details on the  
40 method have been elaborated in the supplement.

In terms of the values of IF, the magnitude of IF changes from different observation sites based on our past experience. And from Fig. 6 in the manuscript, it can be seen that the absolute values of IF increase with higher levels, which implies that there is no universal criteria for the identification of intermittency using IF. However, we can extract a reference value for these two cases in Tianjin in this study. The following figure (also Fig.7 in the revision) illustrates the relationship between IF and  $u_*$  and nocturnal  $z/L$ . The absolute IF increases with stronger turbulent strength when stability in the ABL becomes weaker. Hence, a point of intersection can be identified using the fittings from least-squares regression and represent a critical IF value at given level (here 40 m) beyond which the intermittency of turbulence in the ABL is significant. Based on the regression analyses, the cross points correspond to IF values of -0.53 (Case-1) and -0.50 (Case-2), respectively. Hence, in the present study, we adopt -0.5 as a threshold for the strong intermittency in the ABL. Some relative discussion has added to the revision.

“Besides, the points of intersection from the least-squares regression in Fig. 7 could denote the threshold beyond which the intermittency of turbulence arises under the mutual influence of dynamic and thermodynamic. The values of IF are -0.52 and -0.50 for Case-1 and Case-2, respectively. Hence, a cut-off value of IF (-0.50) can be identified to manifest the significant intermittency of turbulence. But it should be kept in mind that the absolute values of IF change from different heights and sites and this cut-off value of IF can only be used as a reference in the present study.” (page 13 lines 12-16)

“For 40 m, a cut-off value of IF (-0.50) indicates the initiation of strong turbulent intermittency in the ABL, while this is not a universal value and the threshold varies with different cases.” (page 18 lines 4-6)

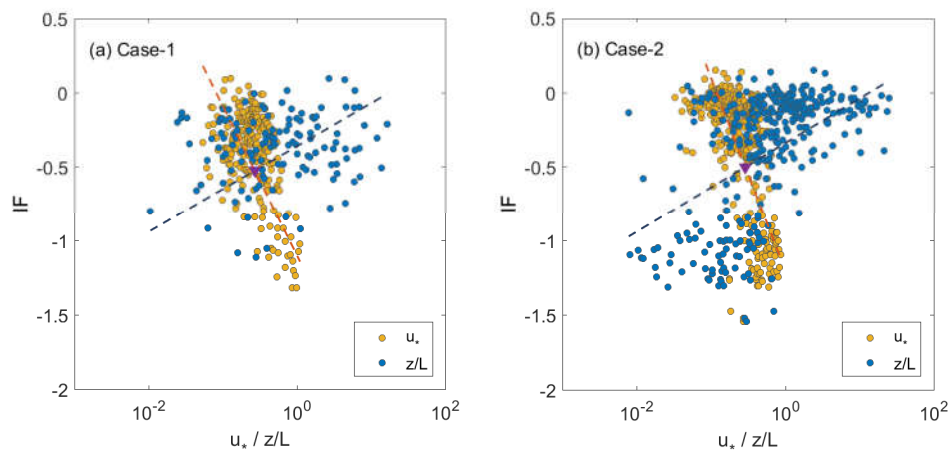


**Figure 7 in the manuscript.** Scatter plot of IF vs.  $u_*$  and  $z/L$  (night time) for (a) Case-1 and (b) Case-2 at 40 m. The dashed lines are the fittings from least-squares regression and the triangle marks the cross point.

The discussion of Figure 5 in the beginning of page 11 is a bit confusing. The authors state that the

difference for CSs is much more obvious. I do not understand this statement. By looking at the figure, the differ curves for TS show more spread than the curves for CS. So what are the authors referring to when discussion about differences?

Also, figures 5a-d have the straight line for fully developed turbulence (faint solid black lines). This line should show up more clearly in the figure and it should be said that it is a solid line.

**Response:** Thank you so much for your detailed comments. Yes, the beginning of page 11 should be “TSs”. We apologize for this slip of the pen and have corrected it in the revision. Please see page 10 lines 3-4: “However, the difference for TSs is much more obvious (in Figs. 5b and 5d), indicating stronger intermittency in the turbulence.”

Also, bolder lines for  $q/3$  are used in Fig.5 and the caption has been written as “the black solid line”.

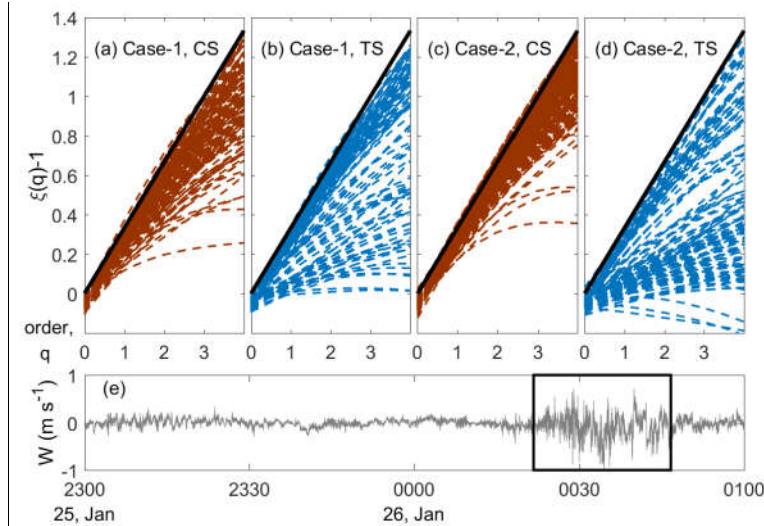


**Figure 5 in the manuscript.** Hilbert-based scaling exponent function at 40 m during different stages for (a) – (b) Case-1 and (c) – (d) Case-2, where each dashed curve represents the result of 30-min vertical wind speed signal and the black solid line denotes the K41 result  $q/3$ . (e) compares vertical wind fluctuation at 40 m between the CS (before 00:00 on 26 January 2017) and TS (after 00:00 on 26 January 2017). The latter shows apparent ‘bursts’ marked by the rectangular frame.

Please check out that all the used mathematical symbols are explained in the text.

**Response:** Thank you. We have checked through the text and defined all of the mathematical symbols.

A few grammatical issues:

Page 1, line 25 should read "particulate matter"

Page 14, line 7: . . .we summarize. . .

**Response:** We are sorry for these mistakes and have been corrected them.

### Response to Referee #3

Dear reviewer,

5 We really appreciate your revealing questions and comments. Some key points about the intermittent turbulence in the SBL that you have brought up with are helpful to improve this work. We also thankful for the useful references you suggested. We did our best to respond to these comments one by one. We hope the reviewer would approve of our following response.

10 Normally, intermittent turbulence is associated with the stable boundary layer (SBL). That is, turbulence strength varies when the background stratification is generally stable. When the stratification is totally wiped out by strong turbulent mixing for a relatively long period, the relatively strong turbulent mixing is not considered as part of a time series of intermittent turbulent mixing anymore. In this study, a period of strong turbulent mixing occurred at the end of all the three cases and each of them lasted for nearly a day. If the authors think the strong turbulent mixing period in each case is part of the time series of intermittent turbulence, this is definitely not what intermittent turbulence in the traditional definition.

15 **Response:** We really appreciate your questions. As your comments note, intermittent turbulence in the SBL is manifested by sporadic bursts lasting from tens of seconds to several minutes. In this study, turbulence during TSs is much stronger than that of CSs and after checking through all of the raw time series, we find that vertical wind speed during TSs is characterized by episodic and intermittent events. The primary reason of the seemingly continuous turbulence during TSs in Fig.2 is that the 10-Hz observed turbulence is confined to a narrow plot and the weak events are covered by the relatively stronger fluctuations, which makes it look like continuous. For space reasons, here we take three examples to illustrate the details of intermittent turbulence during the TSs, one for Case-1 and the other two for Case-2. Meanwhile, the intrinsic mode functions (IMFs) from the empirical mode decomposition are given. As shown in the following Figure 1, the raw time series of vertical wind speed are not fully-developed and continuous. On the contrary, the strength of turbulence is variable. The stronger turbulence can last several minutes and frequently happens within each time series (marked by shaded areas). And this characteristic is more obvious in the high frequent IMFs (i.e. from IMF1 to IMF8). These results show that the relatively stronger turbulence during TSs happens intermittently but not continuously. Some previous observations also confirmed that intermittent bursts of turbulence and mixing can also occur multiple times (Poulos, et al., 2002). We suppose that the intermittent turbulence during TSs in Fig. 2 is just covered by the frequently happened bursts.

20

25

30



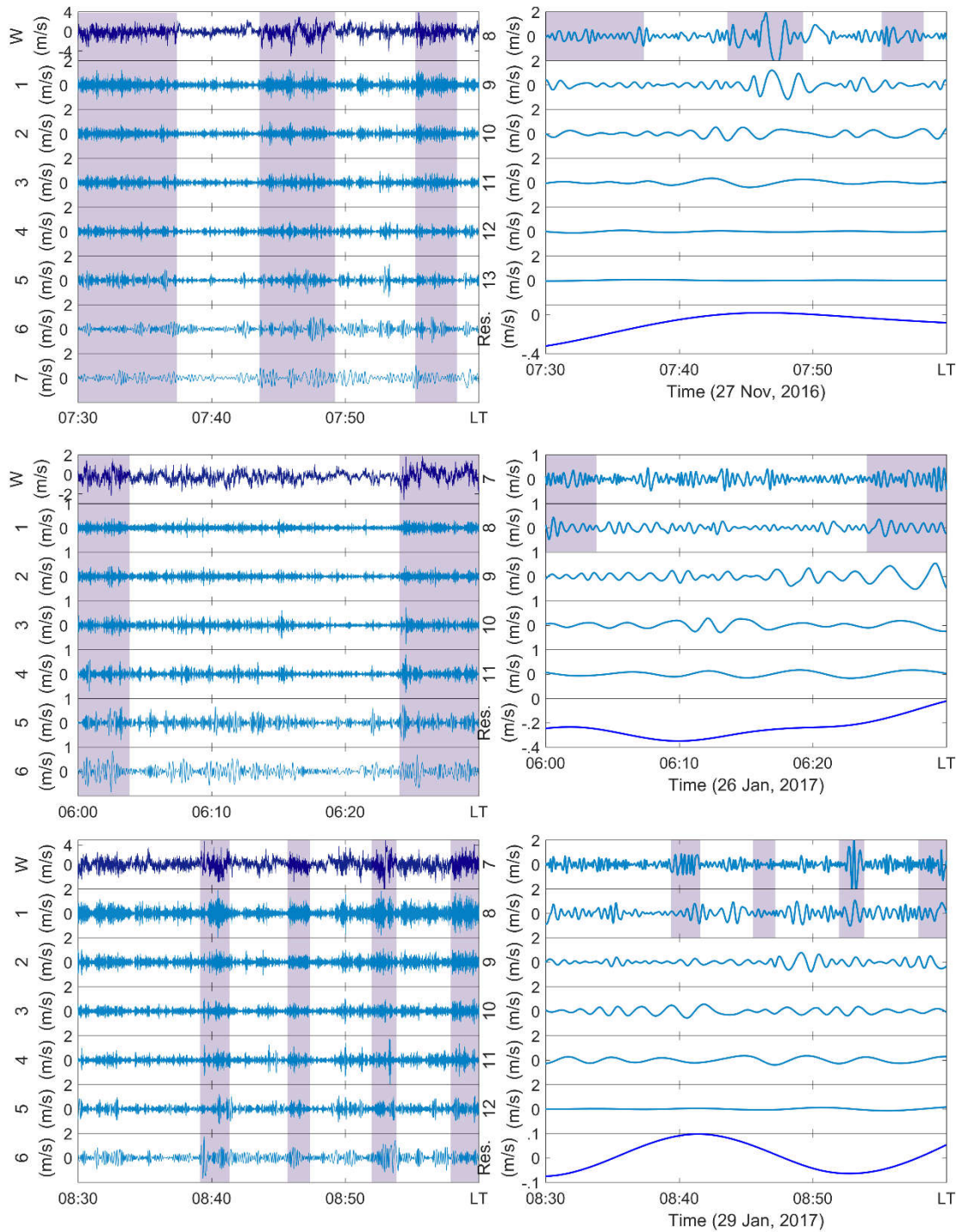


**Figure 1** Three examples of IMFs and 30-min vertical wind speed from TSs. The shaded areas mark the relatively strong intermittent “burst”.

Meanwhile, we use some other indexes, including kurtosis and FI (Flux Intermittency defined by Mahrt, 1998), to verify the behavior of intermittency. The normalized probability density function of fully-developed turbulence should be Gaussian but intermittency would modify its shape. Therefore, kurtosis ( $K = \overline{u'^4}/\sigma^4$ ) that characterizes the variation of probability distribution could be introduced as an intermittency index (Vindel et al., 2008). Another useful index for intermittency is FI, which is shorthand for flux intermittency proposed by Mahrt (1998) and has been applied in many works (e.g. Ha et al., 2007). FI is defined as  $\sigma_F/|F|$ , where  $\sigma_F$  is the standard deviation of the averaged friction velocity and  $|F|$  is the absolute value of friction velocity. Considering the limited scale in the SBL,  $\sigma_F$  is based on 1-min values of friction velocity and  $|F|$  is 30-min averaged. Figure 2 presents Kurtosis and FI, compared with simultaneous  $PM_{2.5}$  concentration and IF. It can be seen that the values of Kurtosis and FI are much larger during TSs, which is consistent with the development of  $PM_{2.5}$  concentration and IF values. All of the parameters confirm that, the relatively stronger turbulence during TSs is intermittent but not fully-developed. Besides, it should be noticed that the small values of turbulence during CSs are mainly due to the extremely weak turbulent fluctuation. Considering that the objective of this work is not the comparison between different methods, we just applied the arbitrary-order HSA technique into this study. According to Huang et al. (1998), this method is intuitive, direct, and adaptive, with a posteriori-defined basis, from the decomposition method, based on and derived from the data, which makes it suitable for the analysis of nonlinear and non-stationary turbulence signals in the ABL. Detailed discussion on the methodology is given in the supplement.

The results of Kurtosis and FI have been added to verify the conclusion as in:

“In order to validate the results of IF, another two parameters to indicate the intermittency of turbulence were developed using the same data: one is kurtosis (Vindel et al., 2008) and the other is FI (Mahrt, 1998; Ha et al., 2007). The results of both kurtosis and FI are consistent with those of IF (see Figure S7).” (page 13, line25, lines 3-6)

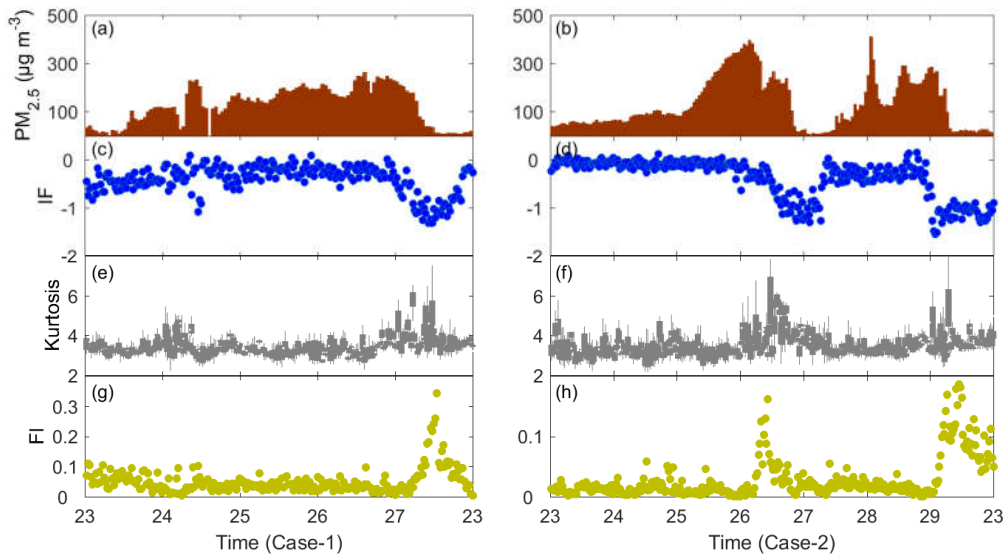


**Figure 2** Comparison of (a) – (b)  $PM_{2.5}$  concentration, (c) – (d) IF, (e) – (f) Kurtosis, and (g) – (h) FI by Mahrt (1998). Left panel is for Case-1 and right panel is for Case-2.

5

Physically, intermittent turbulent mixing in the SBL can be generated by intermittent strengthening wind shear, which can be associated with low level jets (LLJs) as pointed by the authors in the paper. However, this mechanism is not new; Banta et al. (2003, JAS; 2006, QJ; 2007 JAS) have investigated relationships between LLJs and turbulent mixing extensively.

10

**Response:** Yes, a series of works have focused on the relationship between the LLJs and intermittent turbulence, which is a widely-accepted mechanism. Based on this mechanism, we further attempted to reveal the effect of intermittent turbulent mixing on the dispersion of  $PM_{2.5}$  from a viewpoint of small-scale turbulent structure. As far as we know, there is few works aiming on this topic and we hope this study could provide a different new angle to think about the possible reasons for the dispersion of near surface  $PM_{2.5}$ . We are also thankful for your useful references. These works enhanced our understanding on the LLJs and intermittent turbulence and we cited these works in the revision.

15

20

“The reasons for intermittent turbulence in the ABL have not yet been well understood. Some potential causes include gravity waves (Sorbján and Czerwinska, 2013; Strang and Fernando, 2001), solitary waves (Terradellas et al., 2005), horizontal meandering of the mean wind field (Anfossi et al., 2005), and low-level jets (LLJs, Marht, 2014; Banta et al., 2007; 2006; 2003).” (page 15, lines 2-5)

25

In addition, from the title of the paper, it seems that the authors would address the role of intermittent turbulent mixing to the vertical dispersion (not diffusion, diffusion is for molecular movements) of  $PM_{2.5}$ . However, the observation indicates that the intermittent turbulent mixing during the high  $PM_{2.5}$  period is not strong enough to disperse  $PM_{2.5}$  and the significant reduction of  $PM_{2.5}$  is observed at the

end of each event when strong mixing arrives. Then what is the significance of intermittent turbulence during the stable period? What is the significance of the new intermittent turbulence index introduced here in comparison with simple parameters such as wind speed if wind shear is the key physical process for dispersing PM<sub>2.5</sub>?

5 **Response:** Thank you so much for your comments. The title is changed into “Intermittent turbulence contributes to vertical dispersion of PM<sub>2.5</sub> in the North China Plain: cases from Tianjin” in the revision. And we have checked through the paper to rewrite “diffusion” with “dispersion”. We are sorry for the ambiguity. Actually, the turbulence during TSs belongs to intermittent regime while the CS can be considered as a more stable regime and the turbulence is largely suppressed.  
10 The turbulence during CSs is too weak with mean  $u^*$  and TKE less than 0.3 m/s and 0.5 m<sup>2</sup>/s<sup>2</sup> respectively, and  $z/L$  during the nighttime is much larger than 1, which could be sorted as the extremely stable regime or radiation regime (as in Mahrt, 2014). On the other hand, the turbulence of the TS is relatively stronger but not strong enough. These are two totally different stratification conditions. In order to reveal the distinction of different stages and the corresponding turbulence, an index (IF) was proposed. According the theory of arbitrary-order HSA, the larger deviation of scaling exponent  $\xi(q)$  represents stronger intermittency of turbulence. At this point, the turbulence during TSs is intermittent, according to the distribution of IF (Fig.6). On the contrary, the values of IF during CSs are near zero, which is mainly attributed to extremely weak fluctuation ( $u_*$  less than 0.3 m/s). To avoid ambiguity, the time with  $u_* < 0.3$  m/s is colored as grey in Fig.6. As mentioned  
20 in the first response above, the results of other indexes (i.e. kurtosis and FI) also confirm the conclusion in this study, that is, the turbulence during TSs is intermittent and the associated intermittent turbulent mixing facilitates the dispersion of PM<sub>2.5</sub> near the surface. We emphasized this in the revision:

25 “The results show that the turbulence is very weak during the cumulative stage due to the suppression by strongly stratified layers; while for the stage of dispersion, the turbulence is highly intermittent and not locally generated.” (page 1 lines 20-22)

30 “Any of these mechanisms would destroy the statistical symmetries stored in the fully developed turbulence, resulting in deviations from K41’s  $q/3$  and a set of concave curves in which the degree of the discrepancy of concave curves manifests the strength of turbulent intermittency.” (page 11 lines 21-22 and page 12 lines 1-2)

“The Hilbert-based exponent scaling function  $\xi(q)$  shows great deviations from K41’s theoretical result of  $q/3$  by a set of concave curves, indicating that the enhanced turbulence in the ABL when entering the TS is intermittent rather than continuous or fully developed.” (page 17 lines 18-20)

35

Furthermore, because the stable boundary layer is known to be associated with weak winds when wind direction variations can be significant, how does wind advection contribute to the temporal variation of PM<sub>2.5</sub> besides vertical dispersion of PM<sub>2.5</sub> by turbulent mixing? Where is the high PM<sub>2.5</sub> source?

40 **Response:** Thank you for your questions. PM<sub>2.5</sub> pollution in Tianjin and its neighboring cities (i.e., Beijing) has received great attention and a series of works have studied the impacts of synoptic and local circulation (Zhang et al., 2017; Miao et al., 2017; Ye et al., 2016; Zhang et al., 2012; Zheng et al., 2015a; Jiang et al., 2015). Here we summary their main conclusions. Tianjin is located in one

of the most polluted city clusters (the so-called Beijing-Tianjin-Hebei region, BTH region) and surrounded by Hebei, western Shandong and northern Henan, several most severely polluted provinces in Northern China (see map in Figure 3). Therefore, southerly flows from the polluted areas would deteriorate the air quality in Tianjin (Zhang et al., 2017; Miao et al., 2017; Zheng et al., 2015a; Jiang et al., 2015). Tianjin features a four-season climate and is under the influence of the Siberian anticyclone in winter. The strong north-westerly wind from the Siberian anticyclone in winter is helpful to the advection of air pollutants. Therefore, the clean days are associated with the high-pressure centers northwest of the polluted region. In order to summarize the circulation mechanism, Fig.2 also illustrates the wind vector during these two cases. Please see page 7 line 14-20:

“For Case-1, wind at lower levels mainly comes from the south-east during the CS, while the dominant wind direction turns into west when it comes to the TS. Although the wind direction for Case-2 is seemingly unsteady in Fig. 2, the statistical the rose diagrams (see Figure S8) confirm a similar result, with south-easterly flows dominating the CS and westers for the TS. This wind-direction pattern is in agreement with previous works (Zhang et al., 2017; Miao et al., 2017; Zheng et al., 2015a; Jiang et al., 2015). They found that south-easterly wind can bring the aerosols emitted by the surrounding cities to this region while the clean hours are normally characterized by strong high-pressure centers northwest of the polluted region in winter.”

Some works (Zhang et al., 2017; Wang et al., 2014) have revealed that regional transport and local emission both play an important role in air quality in the BTH region. One work by Zhang et al., (2017) focusing on the primary  $PM_{2.5}$  found that in Tianjin, primary  $PM_{2.5}$  mainly originated from local emission before heavy pollution events; when it comes to polluted periods, the contribution from non-local region increased and amount of pollutants were transported from Shandong, Henan, even Jiangsu and Anhui via the low-level southerly flows. In addition, some works (Zheng et al., 2015a; Chan and Yao, 2008) have pointed out that if a large-area pollution event occurred in densely distributed mega-cities (as in BTH region), air pollution might not be eliminated solely by advection considering that the up-wind flows are polluted as well. Based on these solid results by previous works, this work tries to reveal the effects of the vertical transport of intermittent turbulence which is a relatively new and different view so far.

“However, in the region with densely distributed mega-cities (as in the case of Tianjin), because the upwind flows is polluted, mere advection may not be enough to disperse pollutants, thus resulting in persistent air pollution events (Zheng et al., 2015a; Chan and Yao, 2008).” (page 7 lines 20-22)

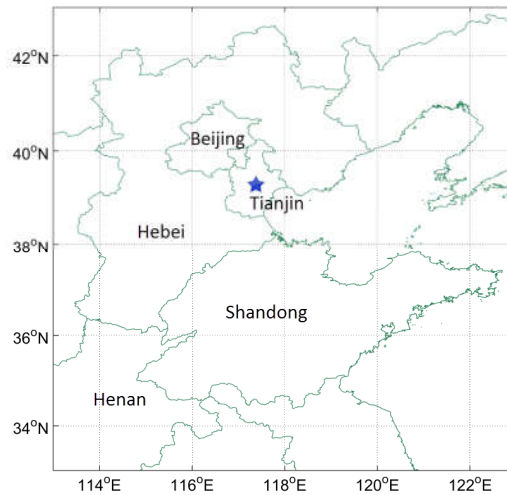


**Figure 3** Map of Tianjin and its surrounding cities.

## 5 References

- Chan, C. K., & Yao, X. (2008). Air pollution in mega cities in China. *Atmospheric environment*, 42(1), 1-42.
- Ha, K. J., Hyun, Y. K., Oh, H. M., Kim, K. E., & Mahrt, L. (2007). Evaluation of boundary layer similarity theory for stable conditions in CASES-99. *Monthly Weather Review*, 135(10), 3474-3483.
- Huang, N. E., Shen, Z., Long, S. R., Wu, M. C., Shih, H. H., Zheng, Q., ... & Liu, H. H. (1998). The empirical mode decomposition and the Hilbert spectrum for nonlinear and non-stationary time series analysis. In *Proceedings of the Royal Society of London A: mathematical, physical and engineering sciences*, 454(1971), 903-995.
- Mahrt, L. (1998). Nocturnal boundary-layer regimes. *Boundary-layer meteorology*, 88(2), 255-278.
- Mahrt, L. (2014). Stably stratified atmospheric boundary layers. *Annual Review of Fluid Mechanics*, 46, 23-45.
- Poulos, G. S., Blumen, W., Fritts, D. C., Lundquist, J. K., Sun, J., Burns, S. P., ... & Terradellas, E. (2002). CASES-99: A comprehensive investigation of the stable nocturnal boundary layer. *Bulletin of the American Meteorological Society*, 83(4), 555-581.
- Vindel, J. M., & Yagüe, C. (2011). Intermittency of turbulence in the atmospheric boundary layer: Scaling exponents and stratification influence. *Boundary-layer meteorology*, 140(1), 73-85.
- Wang, Z., Li, J., Wang, Z., Yang, W., Tang, X., Ge, B., ... & Wand, W. (2014). Modeling study of regional severe hazes over mid-eastern China in January 2013 and its implications on pollution prevention and control. *Science China Earth Sciences*, 57(1), 3-13.
- Zhang, Y., Zhu, B., Gao, J., Kang, H., Yang, P., Wang, L., & Zhang, J. (2017). The source apportionment of primary PM<sub>2.5</sub> in an aerosol pollution event over Beijing-Tianjin-Hebei region

using WRF-Chem, China. *Aerosol and Air Quality Research*, 17, 2966-2980.

Zheng, G. J., Duan, F. K., Su, H., Ma, Y. L., Cheng, Y., Zheng, B., ... & Pöschl, U. (2015). Exploring the severe winter haze in Beijing: the impact of synoptic weather, regional transport and heterogeneous reactions. *Atmospheric Chemistry and Physics*, 15(6), 2969-2983.

- 5 Zheng, G. J., Duan, F. K., Su, H., Ma, Y. L., Cheng, Y., Zheng, B., Zhang, Q., Huang, T., Kimoto, T., Chang, D., Pöschl, U., Cheng, Y. F. and He, K. B.: Exploring the severe winter haze in Beijing: The impact of synoptic weather, regional transport and heterogeneous reactions, *Atmos. Chem. Phys.*, 15(6), 2969–2983, doi:10.5194/acp-15-2969-2015, 2015a.



## List of relevant changes in the manuscript

- 5 **Change 1.** The title is changed into “Intermittent turbulence contributes to vertical dispersion of PM<sub>2.5</sub> in the North China Plain: cases from Tianjin”.
- Change 2.** The advantages and process of the arbitrary-order HSA technique is rewritten in the revision, especially the derivation of IF index. Besides, a supplement is attached to elaborate the details on the arbitrary-order HSA, including some basic background information, figures, and references.
- 10 **Change 3.** The criteria of quality control is rewritten.
- Change 4.** The development of inversion layer and boundary layer height is given and discussed based on the tower observation and WRF model simulation results.
- 15 **Change 5.** The behavior of intermittent turbulence is rewritten and specified in the revision. That is, the turbulence during TSs is intermittent, which enhances the vertical turbulent flux and contributes to the dispersion of pollutant particles near the surface. While the turbulence during CSs is too weak and strongly suppressed by the stable stratification, which can be considered as the extremely stable regime or radiation regime. Some other indexes for intermittency (kurtosis and FI by Mahrt, 1998)
- 20 are given in the supplement to verify the results of IF in this work.
- Change 6.** The importance of synoptic and local circulation is addressed in the revision. Considering this topic has been studied by many previous works, we discuss the impacts of horizontal advection based on the wind vector observation and cite several key references.
- 25 **Change 7.** A comparison between IF and other variables (i.e.  $u^*$  and  $z/L$ ) is added as Fig. 7. And a cut-off value of IF (-0.50) is developed to indicate the initiation of strong turbulent intermittency in the ABL.
- 30 **Change 8.** Some important references are cited, including LLJs, local circulation, and pollutant source.

# Intermittent turbulence contributes to vertical ~~diffusion~~-dispersion of PM<sub>2.5</sub> in the North China Plain: cases from Tianjin

Wei Wei<sup>1</sup>, Hongsheng Zhang<sup>2</sup>, Bingui Wu<sup>3</sup>, Yongxiang Huang<sup>4</sup>, Xuhui Cai<sup>5</sup>, Yu Song<sup>5</sup>, Jianduo Li<sup>1</sup>

<sup>1</sup>State Key Laboratory of Severe Weather, Chinese Academy of Meteorological Sciences, Beijing 100081, P.R. China

<sup>2</sup>Laboratory for Climate and Ocean-Atmosphere Studies, Department of Atmospheric and Oceanic Sciences, School of Physics, Peking University, Beijing 100081, P.R. China

<sup>3</sup>Tianjin Municipal Meteorological Bureau, Tianjin 300074, P.R. China

<sup>4</sup>State Key Laboratory of Marine Environmental Science, Xiamen University, Xiamen 361005, P.R. China

<sup>5</sup>State Key Joint Laboratory of Environmental Simulation and Pollution Control, Department of Environmental Science, Peking University, Beijing 100081, P.R. China

Correspondence to: Hongsheng Zhang (hsdq@pku.edu.cn)

**Abstract.** Heavy particulate pollution events have frequently occurred in the North China Plain over the past decades. Due to high emissions and poor ~~diffusion~~-dispersion conditions, issues become increasingly serious during cold seasons. Although early studies have explored some potential reasons for air pollutions, there are few works focusing on the effects of intermittent turbulence. This paper draws upon two typical PM<sub>2.5</sub> (particulate matters with diameter less than 2.5 mm) pollution cases from the winter of 2016–2017. After several days of gradual accumulation, the concentration of PM<sub>2.5</sub> near the surface reached the maximum as a combined result of strong inversion layer, stagnant wind and high ambient humidity and then sharply decreased to a very low level within a few hours. In order to identify the strength of turbulent intermittency, an effective index, called Intermittency Factor (IF), was proposed by this work. The results show that the turbulence is very weak during the cumulative stage due to the suppression by strongly stratified layers; while for~~during~~ the stage of ~~diffusion dispersion, the turbulence~~ is highly intermittent and not locally generated. The vertical characteristics of IF and wind ~~field~~ profiles confirm the generation and downward transport of intermittent turbulence from the wind shear associated with low-level jets. The intermittently turbulent fluxes contribute positively to the vertical ~~dispersion-transport~~ of particulate matters and improve the air quality near the surface. This work brought up a possible mechanism of how intermittent turbulence affects the ~~diffusion-dispersion~~ of particulate matters.

## 1 Introduction

In the winter of 2016–2017, severe air pollution events haunted the North China Plain, affecting more than 1/5 of the total population in China (Ren et al., 2017). Particulate pollution, especially PM<sub>2.5</sub> (particulate matters with diameter less than 2.5 mm) pollution, has become the foremost problem, considering its adverse impacts on human health (Dominici et al., 2014; Nel, 2005; Thompson et al., 2014; Zheng et al., 2015b).

Naturally, researchers are alarmed by these issues and want to understand the potential reasons. Some works (Wang et al., 2010; Zhang et al., 2016) reveal the effects of the increasing consumption of fossil fuel and the production of secondary pollutants. Meanwhile, it is reported that climate change (Yin et al., 2017; Yin and Wang, 2017) and synoptic circulation (Zhang et al., 2017; Miao et al., 2017; Ye et al., 2016; Zhang et al., 2012; Zheng et al., 2015a; Jiang et al., 2015) are of great importance in the transport of pollutants as well. Air pollution is essentially a phenomenon of the atmospheric boundary layer (ABL) and is strongly affected by the thermodynamic and dynamic structure of the ABL (Bressi et al., 2013; Gao et al., 2016; Tang et al., 2016). The spatial and temporal structures of turbulent motions have a dominant influence on the local air quality from the hourly scale to the diurnal scale (Shen et al., 2017). However, most of the works (Petäjä et al., 2016) focus on the feedback between aerosol, turbulent mixing and boundary layer, with little discussion on the dynamic effect of turbulence on the transport of particulate matters, not to mention the intermittent turbulence under strongly stable conditions. In fact, severe particulate pollutions tend to frequently occur in cold seasons in northern China (Sun et al., 2004; Zhang and Cao, 2015), during which the stratification of the ABL is more stable (Wang et al., 2017) and the turbulent mixing is relatively weak and intermittent in both temporal and spatial scales (Klipp and Mahrt, 2004; Mahrt, 2014). A series of works (Helgason and Pomeroy, 2012; Noone et al., 2013; Vindel and Yagüe, 2011) have confirmed that the intermittent turbulence accounts for a large amount of the vertical momentum, heat and mass exchange between the surface and the upper boundary layer, implying that intermittent turbulence may be one of the key factors in the pollutant dispersion.

The intermittency of velocity fluctuations comes in bursts (as shown in Figure 2 in Frisch, 1980), which means that turbulent intermittency is non-stationary and has no specific time scale. Moreover, the turbulence in the ABL is inherently nonlinear (Holtslag, 2015) and has complex interaction with other motions, such as low-level jets, gravity waves, solitary waves and other non-turbulence motions (Banta et al., 2006; Sun et al., 2015; Terradellas et al., 2005). To date, different methods have been applied to describe the levels of intermittency, such as the flatness (Frisch, 1995), FI index (Flux Intermittency, Eq. (9) in Mahrt, 1998), wavelet analysis (Salmond, 2005) and so on. Given the non-linearity and non-stationarity of intermittent turbulence in the ABL, we conduct our study using a new technique, the so-called arbitrary-order Hilbert spectral analysis (arbitrary-order HSA, Huang et al., 2008), which has been successfully applied into the analyses of turbulence (Huang et al., 2009, 2011; Schmitt et al., 2009; Wei et al., 2016, 2017). It should be noticed that, the target of this work is not to compare the cons and pros of different methods but to study the turbulent intermittency in the ABL with the help of an effective method. The methodology is generalized and the advances are clarified in Sect. 2.2.

Based on these considerations, this work mainly aims at:

- 1) quantifying the turbulent intermittency in the ABL using the arbitrary-order HSA technique;
- 2) revealing a possible mechanism of the ~~diffusion-dispersion~~ of near-surface PM<sub>2.5</sub> from a viewpoint of intermittent turbulence.

In the following text, the data and method are introduced in Sect. 2, ~~respectively~~. Then Sect. 3 discusses our results in detail, including an overview of the cases, the behavior of turbulence intermittency and its contribution to the pollutant transport. The last Sect. 4 is a conclusion.

## 2 Data and Method

### 2.1 Observation

Tianjin (39.00 °N, 117.21°E, altitude 3.4 m) is the largest coastal city in the North China Plain with a population of more than 1.5 million, covering an area of 11,300 km<sup>2</sup>. Tianjin is located to the east-southeast of Beijing, the capital of China, and neighbors Bohai Sea to the east (Fig. 1). Due to the rapid urbanization in the past decades, Tianjin has a typical urban underlying terrain.

Observations in this work include three parts: 1) a 255-m meteorological observation tower for the measurement of turbulence; 2) a CFL-03 wind-profile radar (WPR) for the boundary-layer wind field; and 3) a TEOM 1405-DF system for the monitor of particular matters. The 255-m meteorological observation tower is situated in the Tianjin Municipal Meteorological Bureau, equipped with three levels (40, 120, and 200 m) of sonic anemometers (CSAT, CAMPBELL, Sci., USA) operating at a sampling frequency of 10 Hz. In addition, the observation ~~by HMP45C probe~~ (HMP45C, CAMPBELL, Sci., USA) at 15 levels is also used to analyze the behavior of relative humidity (RH) and temperature. The Tianjin Municipal Meteorological Bureau is located in a residential and traffic area and the buildings around the 255-m meteorological observation tower are typically 15-25 m in height (Ye et al., 2014). In order to avoid affecting the residential zone, the CFL-03 boundary-layer WPR is mounted nearly 10 km away from the Tianjin Municipal Meteorological Bureau to the west. The 1405-DF TEOM system is located nearly 2.3 km away from the 255-m tower to the east and installed at a height of 3 m to monitor the surface PM<sub>2.5</sub>. Detailed information is listed in Table 1.

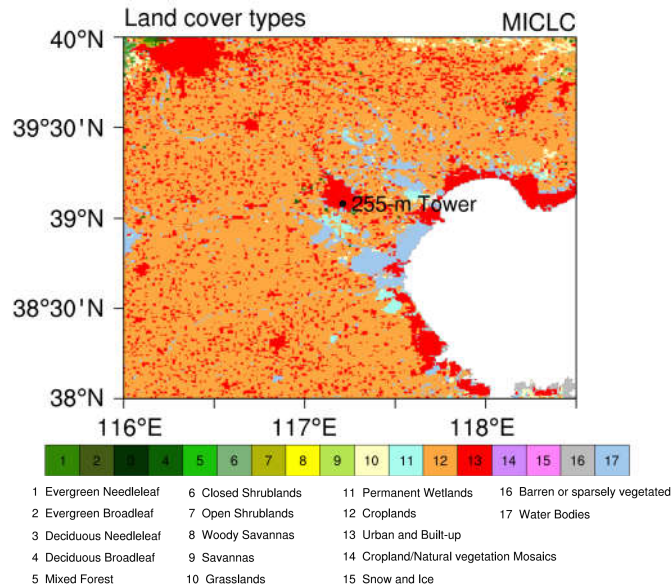


**Figure 1: Landuse map around the site. The black dot denotes the location of the 255-m meteorological observation tower.**

**Table 1. Performance characteristics of instruments**

Instrument	Height	Variables	Sampling resolution	Range	Accuracy
Sonic anemometer-thermometer, CSAT3 <sup>a</sup>	40, 120, 200 m	3-D wind speed <u>(<math>u_x/y/z</math>)</u> , Sonic virtual temperature	0.1 s	$u_x, u_y: \pm 65.536 \text{ m s}^{-1}$ $u_z: \pm 8.192 \text{ m s}^{-1}$ $c^e: 300\text{--}366 \text{ m s}^{-1}$ (-50–60°C)	$u_x, u_y: < \pm 4 \text{ cm s}^{-1}$ $u_z: < \pm 2 \text{ cm s}^{-1}$
HMP45C <sup>a</sup>	15 levels <sup>b</sup>	Temperature, Relative humidity	15 s	-40–60°C 0–100%	$\pm 0.2^\circ\text{C}$ $\pm 2\%$ (<90%) $\pm 3\%$ (>90%)
1405-DF TEOM <sup>c</sup>	3 m	PM <sub>2.5</sub>	1 hr	0–1,000,000 $\mu\text{g m}^{-3}$	$\pm 7.5\%$
CFL-03 boundary layer WPR <sup>d</sup>	< 5,000 m	Horizontal/vertical wind speed ( $U_{h/v}$ ), wind direction	Temporal: 10 min Vertical: 100 m	$U_h: 0\text{--}60 \text{ m s}^{-1}$ $U_v: \pm 20 \text{ m s}^{-1}$ Direction: 0–360°	$U_{h/v}: 0.1 \text{ m s}^{-1}$ Direction: $\leq 10^\circ$

5 <sup>a</sup> CAMPBELL, Sci., USA

<sup>b</sup> 15 levels: 5, 10, 20, 30, 40, 60, 80, 100, 120, 140, 160, 180, 200, 220, and 250 m

<sup>c</sup> Thermo Fisher Scientific, USA

<sup>d</sup> China Aerospace Science & Industry Corp

<sup>e</sup> c is the sound of speed

10

Turbulence observations from the 255-m tower were obtained at a sampling frequency of 10 Hz. Then quality control was applied to all the data (Zhang et al., 2001), such as error flag, spike detection, cross wind correction, spectral loss correction, sonic virtual temperature correction, density fluctuation correction, and coordinate rotation. If more than 20% points within a given 30-min time series were detected as outliers, then this 30-min observation was discarded. An averaging time length of

15

1 min was applied to calculate turbulent fluctuations and fluxes, given the small size eddies under stable conditions. The friction velocity  $u_*$  reads in its form as  $u_* = (\overline{u'^2} + \overline{v'^2})^{1/4}$ , where  $u'/v'/w'$  represent the longitude, lateral and vertical fluctuation of wind vector. The turbulent kinetic energy (TKE) is given by  $\text{TKE} = (\overline{u'^2} + \overline{v'^2} + \overline{w'^2})/2$  and the stability function uses  $z/L = -\kappa z g \overline{w'\theta'}/\overline{\theta} u_*^3$ , in which  $L = -\overline{\theta} u_*^3/\kappa g \overline{w'\theta'}$  is Obukhov length,  $\theta$  is potential temperature, z is observation height, g is gravitational acceleration and  $\kappa$  is von Karman constant with a value of 0.4 here. The data quality of

20

CFL-03 boundary-layer WPR was checked to avoid the effects of poor quality of data. First, data below 200 m were removed due to the interference of surrounding environment, including trees and buildings. Then each vertical profile was

checked through and points with larger than 2.5 standard deviations were regarded as outliers and discarded. A profile was discarded if more than 40% of the data points were outliers or missing (Wei et al., 2014).

Based on an overall consideration of data quality and severity of air quality, two cases happening in the winter of 2016–2017 were identified to study the relationship between intermittent turbulence and pollutant dispersion. The first one persisted for 5 days from 00:00 on 23 November 2016 to 00:00 on 28 November 2016, which is marked as Case-1 for convenience purposes. The second case, that is, Case-2, is from 00:00 on 23 January 2017 to 00:00 on 30 January 2017. All of the time in this work refers to ~~local standard time~~Beijing Time.

## 2.2 Method

- 10 The flow in the ABL is highly nonlinear and non-stationary. In order to deal with the nonlinear and non-stationary time series, we adopted a relatively new technique called the arbitrary-order Hilbert spectral analysis (arbitrary-order HSA, Huang et al., 2008), which is based on the Hilbert-Huang transform (Huang et al., 1998, 1999). The primary reason why the arbitrary-order HSA is used in this work is that this method satisfies locality and adaptivity which are two necessary conditions for the study of nonlinear and non-stationary time series (Huang et al., 1998). ~~On this basis~~Based on the arbitrary-
- 15 order HSA, we proposed an index, called ~~intermittent~~intermittency factor (IF), to quantify the level of turbulent intermittency, which is assumingly more effective compare with some classic quantities. To investigate the effects of vertical mixing in the ~~diffusion~~dispersion of air pollutants, a set of vertical wind fluctuation at 10 Hz obtained by the sonic anemometers (~~CSAT3, CAMPBELL Inc., USA~~) were drawn upon in this study. A brief introduction to the method is mathematically described in this part. For detailed information, one can refer to the work by Huang et al. (2008).
- 20 Firstly, a 30-min vertical wind-speed signal  $X(t)$  is separated into a group of intrinsic mode functions  $C_i(t)$  and a residual  $r_n(t)$  according to the so-called empirical mode decomposition. Here, each intrinsic mode functions  $C_i(t)$  meets two constraints: (i) the difference between the number of local extrema and the number of zero-crossings must be zero or one, and (ii) the running mean values of upper and lower envelopes are zero. The decomposition process is as follows (Huang et al., 1998, 1999):
- 25 1) The first step is to form the upper envelope  $e_{max}(t)$  based on the local maxima of 30-min  $X(t)$  using the cubic spline interpolation. The lower envelope  $e_{min}(t)$  can be constructed following the same method.
- 2) Then, one can define the mean  $m_1(t) = (e_{max}(t) + e_{min}(t))/2$  and the first local signal  $h_1(t) = X(t) - m_1(t)$ .
- 3) So far,  $h_1(t)$  is checked whether it meets the two constraints of intrinsic mode functions. If yes,  $h_1(t)$  is the first intrinsic mode function  $C_1(t) = h_1(t)$  and is taken away from  $X(t)$  to obtain the first residual  $r_1(t) = X(t) - C_1(t)$ .
- 30 Then  $r_1(t)$  is treated as the new signal to begin with step 1). If  $h_1(t)$  does not meet the above constraints, the first step is repeated on  $h_1(t)$  to define the lower and upper envelopes and further the new local detail until  $h_{1k}(t)$  is the first intrinsic mode function  $C_1(t) = h_{1k}(t)$ .

Steps 1–3 are called ‘sifting process’. To avoid over-sifting, the standard deviation criterion (Huang et al., 1998) is applied to stop this decomposition process. After  $n$  times of ‘sifting process’, one obtains a set of  $C_i(t)$  and a monotonic residual  $r_n(t)$ . At this point, the vertical wind fluctuation  $X(t)$  can be expressed as  $X(t) = \sum_{i=1}^n C_i(t) + r_n(t)$ . Then, each mode  $C_i(t)$  is developed to obtain its corresponding analytical signal  $C_i^A(t) = C_i(t) + j\tilde{C}_i(t) = A_i(t)\exp(j\theta_i(t))$  using Hilbert transform (Cohen, 1995), where the imaginary part reads as  $\tilde{C}_i(t) = \frac{1}{\pi} \int_{-\infty}^{\infty} \frac{C_i(\tau)}{t-\tau} d\tau \frac{d\theta_i}{dt}$ , and  $A_i(t)$  and  $\theta_i(t)$  are the instantaneous amplitude and phase. Also, one can define the instantaneous frequency as  $\omega_i(t) = \frac{1}{2\pi} \frac{d\theta_i}{dt}$ .

Note that the instantaneous amplitude  $A_i(t)$  and frequency  $\omega_i(t)$  are both a function of time, which means that a Hilbert spectrum  $H(\omega, t)$  can be defined with  $A_i(t)$  expressed in the space of frequency–time. So does the joint probability density function (p.d.f.)  $p(\omega, A)$ . ~~Then~~ If  $H(\omega, t)$  is integrated with respect to time, one can get  $H(\omega)$  which can be further expressed as  $H(\omega) = \int p(\omega, A)A^2 dA$ . If the power exponent of instantaneous amplitude is extended from 2 to  $q$ , one can define arbitrary-order Hilbert spectrum as  $\mathcal{L}_q(\omega) = \int p(\omega, A)A^q dA$ , where  $q \geq 0$  is the arbitrary moment.

In the case of scale invariance, the arbitrary-order Hilbert spectrum follows  $\mathcal{L}_q(\omega) \sim \omega^{-\xi(q)}$  in the inertial subrange, in which  $\omega$  is the frequency and  $\xi(q)$  is the scaling exponent function. Under the assumption of fully developed turbulence, the distribution of scaling exponent function with the order  $q$  is linear and meets  $\xi(q) - 1 = q/3$ , which is developed from  $\xi(q) = \zeta(q) + 1$  (Huang et al., 2008, 2011), where  $\zeta(q)$  is the scaling exponent function in  $q$ -order structure function  $S_q(l) = \langle (\delta X(l))^q \rangle = \langle (X(l+l_0) - X(l_0))^q \rangle \sim l^{\zeta(q)}$ , in which the angular bracket refers to spatial averaging and  $l$  means distance. This exponent law is in agreement with Kolmogorov’s hypothesis (K41 for short) and any intermittency would result in deviations from the theoretical  $q/3$  (Basu et al., 2004). Based on this, we define an index, ~~called Intermittent Factor~~ (IF), as the deviation from the theoretical value at the maximal order:  $IF = \xi(q_{max}) - 1 - q_{max}/3$ . Due to the limited observation length, the maximal order  $q_{max}$  is up to 4 in this study to avoid the difficulties and errors in the measurements of high-order moments (Frisch, 1995).

It is well acknowledged that the intermittent turbulence under stable conditions is characterized by sporadic bursts in a timescale of order  $O(10)$  to  $O(1000)$  sec. The statistically unsteady turbulence disobeys the assumptions of traditional theories (Poulos et al., 2002). For example, Fourier spectral analysis asks for a linear system and strictly stationary data; and the widely used wavelet transform is suitable for non-stationary signals but suffers when it comes to nonlinear cases (Huang et al., 1998). As one of the most important steps through this method, the empirical mode decomposition separates the original time series into different modes based on its own physical characteristics without any predetermined basis, implying an intuitive, direct, adaptive, and data-based nature. And with the instantaneous information from the Hilbert transform, one can investigate the behavior of local events, which makes the Hilbert-based method more appropriate for the analyses of intermittent turbulence. This Hilbert-based scaling exponent function  $\xi(q)$  has been applied into the analyses of turbulent intermittency in the ABL (Wei et al., 2016, 2017) and shown its effectiveness and validity.



### 3 Results and Discussion

#### 3.1 Overview of Cases

Figure 2 illustrates the time series of different variables for two cases, including surface PM<sub>2.5</sub> concentration, wind vector, temperature, RH, horizontal wind speed, vertical wind speed, friction velocity  $u_*$ , TKE, and stability parameter  $z/L$ . From the distribution of PM<sub>2.5</sub>, it can be seen that the concentration of ~~PM<sub>2.5</sub> pollutants~~ gradually increased to ~~maxima (263  $\mu\text{g m}^{-3}$  for Case-1 and 412  $\mu\text{g m}^{-3}$  for Case-2)~~ a maximum of 412  $\mu\text{g m}^{-3}$  for PM<sub>2.5</sub> and then dropped to a low level within a few hours ~~no matter for Case 1 and Case 2~~. Based on the concentration of PM<sub>2.5</sub>, we can easily divide each case into two periods: one called the cumulative stage (CS) during which ~~the particulate matters accumulates~~ near the surface; the other named as the transport stage (TS) representing the stage when pollutants dissipate (Zhong et al., 2017). At this point, Case-1 can be separated into the CS from 00:00 on 23 November to 06:00 on 27 November 2016 and the TS from 06:00 on 27 November to 00:00 on 28 November 2016. Case-2 experienced two transitions from the CS to TS which happened at 00:00 on 26 January 2017 and at 00:00 on 29 January 2017, respectively. To distinguish these two transitions, the former is marked as Case-2A and the latter is Case-2B. Table 2 compares the values of mean and standard deviation of different variables between CSs and TSs. Generally, the mean concentration of PM<sub>2.5</sub> during the CS is much higher than that for the TS. For Case-1, wind at lower levels mainly comes from the ~~north-south-east~~ during the CS, while the dominant wind direction turns into ~~south-eastwest~~ when it comes to the TS. ~~However, there is no steady wind direction for Case 2. Although the wind direction for Case-2 is seemingly unsteady in Fig. 2, the statistical the rose diagrams (see Figure S8) confirm a similar result, with south-easterly flows dominating the CS and westers for the TS. This wind-direction pattern is in agreement with previous works (Zhang et al., 2017; Miao et al., 2017; Zheng et al., 2015a; Jiang et al., 2015). They found that south-easterly wind can bring the aerosols emitted by the surrounding cities to this region while the clean hours are normally characterized by strong high-pressure centers northwest of the polluted region in winter. However, in the region with densely distributed mega-cities (as in the case of Tianjin), because the upwind flows is polluted, mere advection may not be enough to disperse pollutants, thus resulting in persistent air pollution events (Zheng et al., 2015a; Chan and Yao, 2008).~~

In terms of temperature, it goes through gradual increase over CSs despite of its diurnal change, which can be attributed to two possible reasons. On one hand, the accumulation of air pollutants results in the increase of the optical depth of the atmospheric column. The majority of incoming solar radiation during the daytime is absorbed by the upper air or scattered into different direction. The part of absorbed radiation heats the upper atmospheric layer, thus contributing positively to inversion layer which is helpful to suppress the turbulent mixing in the ABL (Petäjä et al., 2016). On the other hand, the heavily polluted ABL reduces the loss of surface longwave radiation during night, which is analogous to a cloud covered night. In this case, the heated boundary layer develops into stable stratification. Furthermore, Fig. 3 depicts the ~~distribution of Planetary Boundary Layer Height (PBLH) and the change of~~ daily mean potential temperature profiles ~~over the CS~~ at 15 different heights, ~~including change of  $\theta$  over the CS (Fig. 3a–c) / TS (Fig. 3d–f) and the development during the whole polluted event (Fig. 3g)~~. The  $\Delta\theta$  at given height ~~of CSs~~ was calculated by subtracting the value of  $\theta$  on the last day from that

on the first day ~~of CSs~~. And so it does for TSs. For Case-1,  $\Delta\theta$  during the CS at the lowest level (5 m) is only 5.2 K. But for the top level at 250 m,  $\Delta\theta$  is relatively larger with a value of 6.8 K. This result confirms that the warming of upper layers is stronger than that of lower layers, implying an increasingly stably stratified boundary layer during polluted days. Figs. 3b and 3c for Case-2 verify this conclusion as well. On the contrary,  $\Delta\theta$  during TSs (Fig. 3d–f) presents a significant cooling at higher levels, denoting the collapse of inversion layer at the end of the polluted event. Taking Case-1 as an example, Fig. 3g depicts the evolution of inversion layer. It can be seen that the inversion layer was gradually enhanced from 23 to 27 November but quickly depressed on 28 November, which verifies the results of Fig. 3a–f. Fig. 3h illustrates the distribution of PBLH, which is simulated with the Weather Research & Forecasting (WRF) Model (Zheng et al., 2015c). In Fig. 3h, the PBLH for Case-1 gradually decreased and reached its minimum on the night of 26–27 November. Then the PBLH redeveloped to higher than 1,300 m during the daytime of 28 November. Besides, an ambience with high relative humidity (RH) is favorable for the increase of  $\text{PM}_{2.5}$  concentration in the ABL through secondary formation by heterogeneous reactions (Quan et al., 2015; Wang et al., 2012; Faust et al., 2017) and hygroscopic growth (Engelhart et al., 2011; Petters and Kreidenweis, 2008). For Case-1, the RH during the CS keeps high with a mean value of 53% but sharply falls into a very low level once entering the TS. Similar results can be found in Case-2.

During CSs, both horizontal wind and vertical wind are weak, implying unfavorable transport conditions. On the contrary, the strength of horizontal and vertical wind notably increases during TSs. These results are consistent with that of  $u_*$ , showing a total vertical momentum flux with a mean of  $0.25 \text{ m s}^{-1}$  during the CS of Case-1 ( $0.19$  and  $0.29 \text{ m s}^{-1}$  for Case-2). While the values of  $u_*$  are generally larger than  $0.30 \text{ m s}^{-1}$  in the TS of both two cases. According to the classic TKE budget equation (Eq. 5.2.3 in Stull, 1988), the TKE is distinctively produced by the mechanical wind shear near the surface in the TS, resulting in strong turbulent mixing in the ABL, thus more effective transport of air pollutants. Another important term in the TKE budget equation is the buoyant production or consumption. The stability parameter  $z/L$  is used here to quantify the stratification of layers near the surface. Although the values of  $z/L$  are negative during the daytime, nocturnal  $z/L$  during the CS is notably larger than 1, which means that the consumption caused by buoyancy is dominant compared with the weak production by wind shear. The strongly stable stratification near the surface restrains the vertical turbulence mixing. The reduced mixing, together with emissions and production of secondary pollutants, result in a heavily polluted layer near the surface.

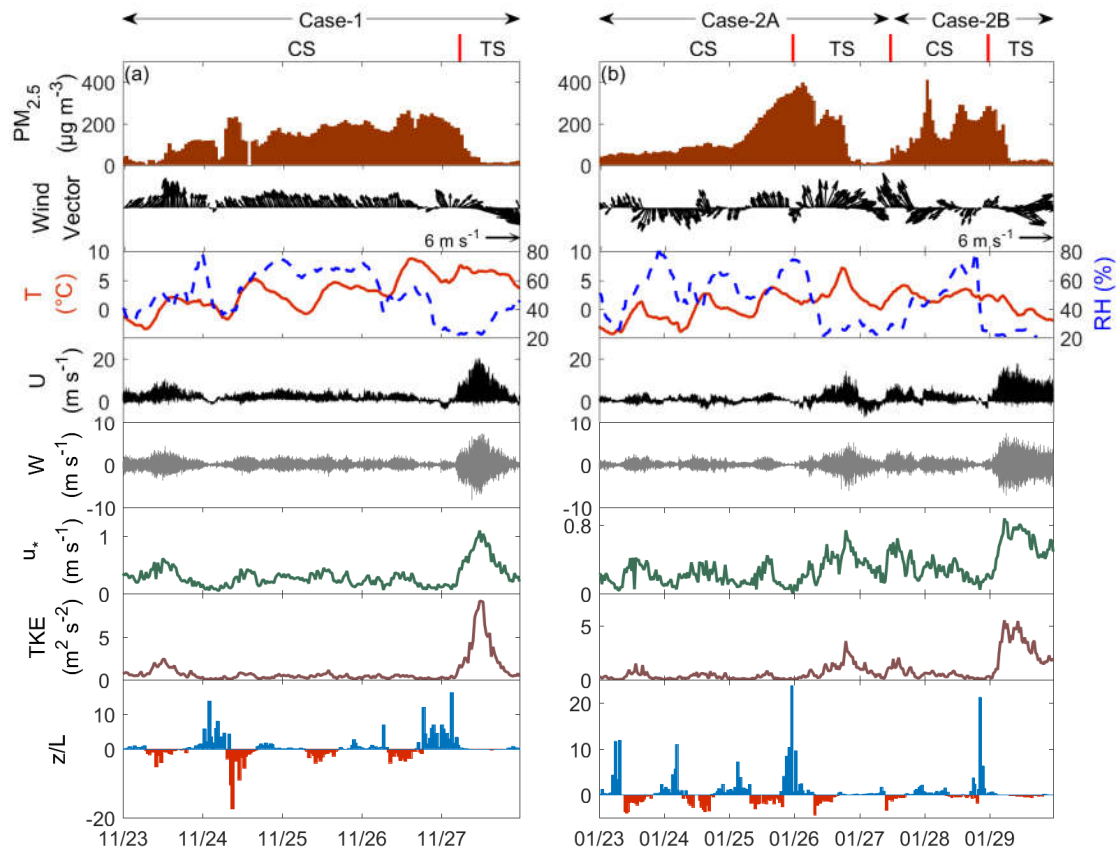
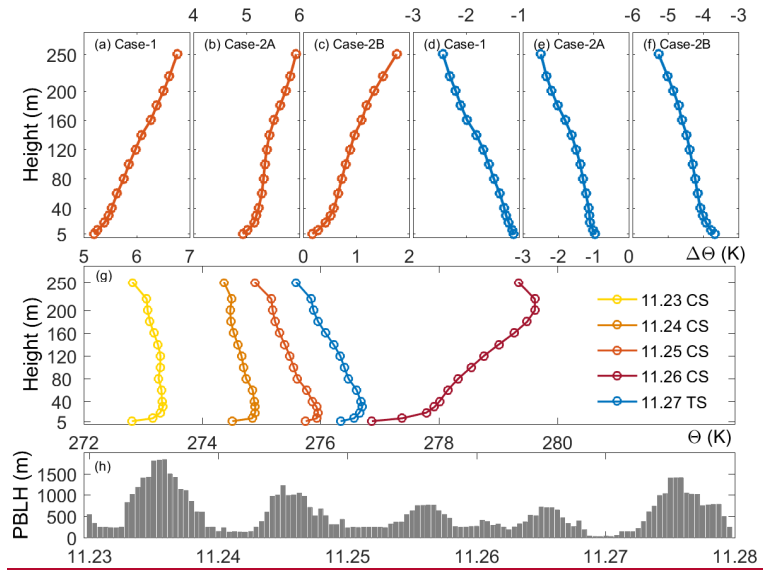


Figure 2. Time series of surface  $PM_{2.5}$ , wind vector, temperature (T), relative humidity (RH), horizontal wind speed (U), vertical wind speed (W), friction velocity ( $u_*$ ), turbulent kinetic energy (TKE), and stability parameter ( $z/L$ ) for Case-1 in (a); for Case-2 in (b). The CS refers to the stage during which pollutants culminated and the TS represents clear days. All of the variables were observed at 40 m except for  $PM_{2.5}$  concentration which is at the surface.



**Figure 3. Vertical distribution of the change of daily mean potential temperature during CSs. Three panels refer to The change of daily mean potential temperature of CSs is showed in (a) Case-1, (b) Case-2A, and (c) Case-2B and (d) – (f) are for TSs. (g) illustrates the evolution of inversion layer of Case-1. (h) is the PBLH simulated with WRF Model.**

5 **Table 2. Mean and standard deviation (Mean  $\pm$  SD) of key variables during different periods**

Variables	CS		TS	
	Case-1	Case-2	Case-1	Case-2
PM <sub>2.5</sub> ( $\mu\text{g m}^{-3}$ )	145 $\pm$ 71	139 $\pm$ 101	31 $\pm$ 35	104 $\pm$ 138
Temperature (K)	275.6 $\pm$ 2.9	272.7 $\pm$ 2.3	279.2 $\pm$ 0.9	275.4 $\pm$ 1.8
RH (%)	53 $\pm$ 15	48 $\pm$ 15	32 $\pm$ 8	35 $\pm$ 17
U ( $\text{m s}^{-1}$ )	1.85 $\pm$ 1.38	0.61 $\pm$ 0.87	3.78 $\pm$ 2.90	1.47 $\pm$ 1.39
Magnitude of W ( $\text{m s}^{-1}$ )	0.28 $\pm$ 0.26	0.23 $\pm$ 0.22	0.61 $\pm$ 0.64	0.36 $\pm$ 0.35
$u_*$ ( $\text{m s}^{-1}$ )	0.25 $\pm$ 0.12	0.19 $\pm$ 0.10	0.59 $\pm$ 0.26	0.33 $\pm$ 0.15
TKE ( $\text{m}^2 \text{s}^{-2}$ )	0.50 $\pm$ 0.43	0.25 $\pm$ 0.71	3.35 $\pm$ 2.81	0.54 $\pm$ 0.42
z/L at night	1.70 $\pm$ 2.74	2.18 $\pm$ 3.74	0.23 $\pm$ 0.21	0.61 $\pm$ 1.43

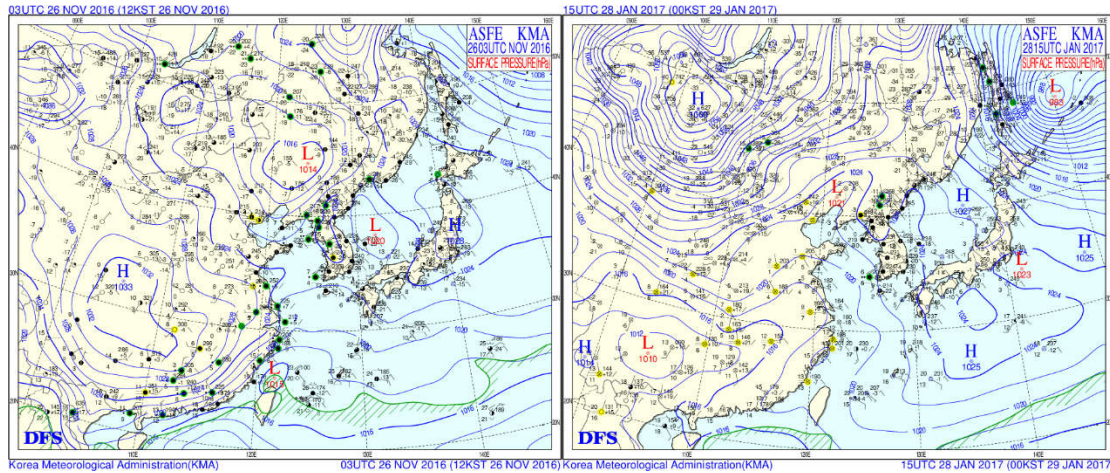


**Figure 4. Typical surface weather condition during CSs. Weather charts are from Korea Meteorological Administration.**

- 5 In addition to the meteorological parameters, synoptic weather conditions also play an important role in the formation and dissipation of heavy air pollutions (Zheng et al., 2015a). Fig. 4 takes two examples from Case-1 and Case-2 to illustrate the typical synoptic weather condition during CSs. In general, the accumulation of pollutants is accompanied by a low pressure system dominating the northern China. Under the control of cyclone system, this region is covered by sparse isobars and is controlled by stagnant wind field, resulting in unfavorable diffusion-transport conditions.

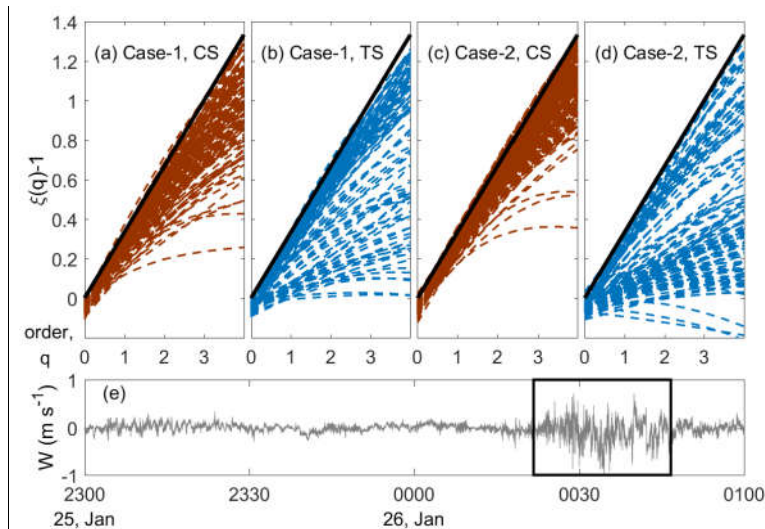
10

### 3.2 Characteristics of intermittent turbulence

15 Considering the nonlinear and non-stationary nature of turbulent intermittency, it is imperative to choose an effective and reliable method before we implement the analyses. The arbitrary-order HSA used in this work to identify IF index meets the necessary conditions for the analyses of nonlinear and non-stationary time series, such as complete, orthogonal, local, and adaptive (Huang et al., 1998). Our previous works (Wei et al., 2016, 2017) have confirmed the validity of arbitrary-order HSA method in the identification of turbulent intermittency in the ABL.

20 As mentioned in Sect. 2.2, if turbulence in the ABL is fully developed, the Hilbert-based exponent scaling function  $\xi(q)$  should follow the linear distribution of  $\xi(q) - 1 = q/3$  (Huang et al., 2008). However, in the real world, there exist all kinds of instability mechanisms on different scales, such as the large-scale baroclinic instability and the small-scale convective instability (Frisch, 1980). Furthermore, under stable conditions, the very low boundary-layer height limit the development of eddies and the stagnant wind near the surface is not enough to maintain the turbulence mixing. Any of these mechanisms would destroy the statistical symmetries stored in the fully developed turbulence, resulting in deviations from K41's  $q/3$  and

a set of concave curves in which the degree of the discrepancy of concave curves manifests the strength of turbulent intermittency. Figs. 5a–5d present the behavior of  $\xi(q) - 1$  at 40 m during different stages from two cases. Compared with the theoretical  $q/3$ ,  $\xi(q) - 1$  from CSs and TSs both shows deviations to some extent. However, the difference for CSs-TSs is much more obvious (in Figs. 5b and 5d), indicating stronger intermittency in the turbulence. Fig. 5e further gives a two-hour example of vertical wind speed during 23:00 on 25 January to 01:00 and 26 January 2017, which covers the transition from the CS to TS in Case-2A. One noticeable feature is that the magnitude of vertical wind fluctuation significantly increases and is marked by strong burst lasting for nearly 25 min from 00:20 to 00:45 on 26 January 2017. On the contrary, the vertical wind speed is relatively weak and steady during the CS. But it should be kept in mind that the small deviations during CSs do not manifest fully developed turbulence but result from the very weak wind speed in the ABL, at which point the wind shear is either absent or not strong enough to generate intermittency (Van de Wiel et al., 2003). The magnitude of vertical wind speed for CSs is generally less than  $0.58 \text{ m s}^{-1}$ . Under extremely stable conditions, the size of eddies may be too small to be detected by sonic anemometers (Mahrt, 2014).



15 **Figure 5. Hilbert-based scaling exponent function at 40 m during different stages for (a) – (b) Case-1 and (c) – (d) Case-2, where each dashed curve represents the result of 30-min vertical wind speed signal and the black solid line denotes the K41 result  $q/3$ . (e) compares vertical wind fluctuation at 40 m between the CS (before 00:00 on 26 January 2017) and TS (after 00:00 on 26 January 2017). The latter shows apparent ‘bursts’ marked by the rectangular frame.**

20 In order to measure the strength of turbulent intermittency at different levels, an index named as IF was proposed by this work. Since IF is defined as the deviation from the theoretical  $q/3$  at the maximal order  $q_{max}$  (here  $q_{max}$  equal to 4, see Sect. 2.2), the larger absolute values of IF indicate stronger turbulent intermittency at given height. Meanwhile, time with magnitude of vertical wind speed at 40 m less than  $0.3 \text{ m s}^{-1}$  is marked to exclude stagnant wind. Fig. 6 illustrates the distribution of IF at three levels, compared with the concentration of  $\text{PM}_{2.5}$  at the surface. Each sharp decline of surface



PM<sub>2.5</sub> concentration is accompanied by the abrupt change in values of IF. And IF at 40 m level is especially in agreement with the accumulation and dissipation of pollutants at the surface. The increasing deviations of IF when entering the TS manifest more intermittent turbulence, thus stronger vertical mixing in the ABL. In order to validate the results of IF, another two parameters to indicate the intermittency of turbulence were developed using the same data: one is kurtosis (Vindel et al., 2008) and the other is FI (Mahrt, 1998; Ha et al., 2007). The results of both kurtosis and FI are consistent with those of IF (see Figure S7). Previous field ~~site~~ results indicate that a significant proportion of vertical fluxes of heat, momentum, and mass under stable conditions come from intermittent bursts (Poulos et al., 2002). Fig. 7 further confirms the relationship between IF and  $u_*$  or  $z/L_*$ , in which dots of strong turbulence ( $u_*$ ) and weak stable stratification ( $z/L_* \approx 0.1$ ) mainly come from the TS. Larger deviation of IF occurs accompanied by increasing turbulent strength when stability in the ABL becomes weaker. That is, intermittent turbulence (marked by large negative values of IF) leads to strong fluxes during the TS. The enhanced turbulent mixing caused by intermittent bursts contributes positively to the vertical transport of pollutants, improving the air quality near the surface. Besides, the points of intersection from the least-squares regression in Fig. 7 could denote the threshold beyond which the intermittency of turbulence arises under the mutual influence of dynamic and thermodynamic. The values of IF are -0.52 and -0.50 for Case-1 and Case-2, respectively. Hence, a cut-off value of IF (-0.50) can be identified to manifest the significant intermittency of turbulence. But it should be kept in mind that the absolute values of IF change from different heights and sites and this cut-off value of IF can only be used as a reference in the present study.

Besides, another feature of IF in Fig. 6 is that the occurrence of abruptly changed IF at different heights is not simultaneous. In general, the higher the level is, the earlier the intermittent turbulence happens and also the greater the deviations of IF are, which implies that the intermittent turbulence is generated at higher levels and then transported downward. We know that, under weakly stable conditions, turbulence in the ABL is continuous in both time and space, which is mainly dominated by wind shear at the surface. But for strongly stable cases, buoyancy prohibits the turbulent mixing, which enhances the surface radiative cooling, thus increasing the stratification of the ABL (Derbyshire, 1999). Such a positive feedback ultimately leads to the decoupling of boundary layer from the underlying surface, that is, the strong stratification prevents the turbulent exchange between the surface and the ABL. This decoupling could be ceased if there exists wind shear above the stable surface layer, at which point turbulence may be generated at upper levels and then transported downward to rebuild the coupling between the atmosphere and the surface (Mahrt, 1999). The decoupling is suddenly interrupted by the descending turbulence, resulting in intermittent bursts near the surface (Van de Wiel et al., 2012). It is reported (Smedman et al., 1995) that this downward transport of turbulence is related to the pressure transport term in the TKE equation, which means that Monin-Obukhov similarity theory is invalid for this case.



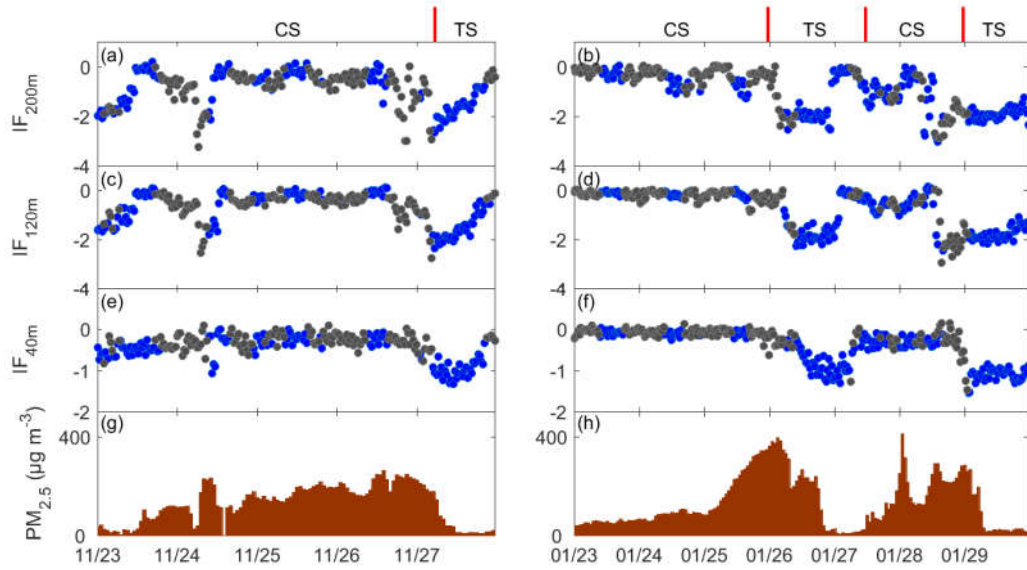


Figure 6. Distribution of (a) – (f) IF at three levels and (g) – (h) concentration of PM<sub>2.5</sub> at the surface. Left panel represents Case-1 and right panel for Case-2. Grey dots denote stagnant wind with vertical wind speed less than 0.3 m s<sup>-1</sup>.

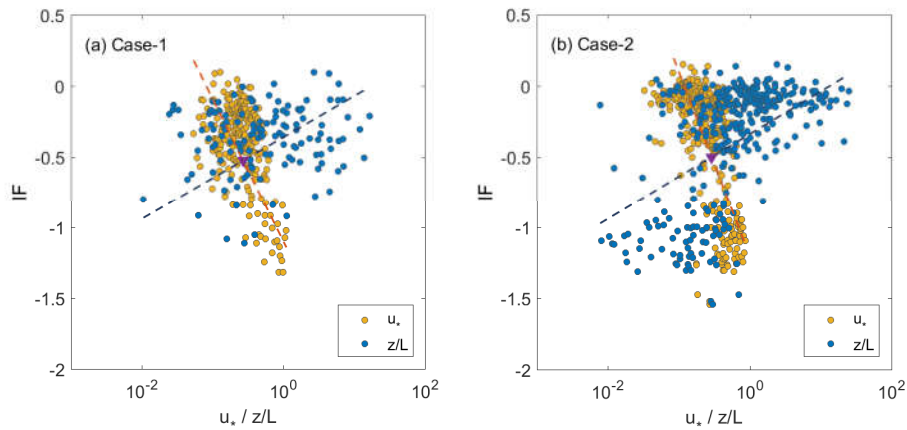


Figure 7. Scatter plot of IF vs.  $u_*$  and  $z/L$  (night time) for (a) Case-1 and (b) Case-2 at 40 m. The dashed lines are the fittings from least-squares regression and the triangle marks the cross point.

### 3.3 Mechanism and transport of intermittency

The reasons for intermittent turbulence under stable conditions in the ABL have not yet been well understood. Some potential causes include gravity waves (Sorbjan and Czerwinska, 2013; Strang and Fernando, 2001), solitary waves (Terradellas et al., 2005), horizontal meandering of the mean wind field (Anfossi et al., 2005), and low-level jets (LLJs, Marht, 2014; Banta et al., 2007; 2006; 2003).

According to the case overview in Sect. 3.1, it can be seen that the stratification of surface layers at night is fairly stable during CSs with values of  $z/L \gg 1$ . Meanwhile, weak  $u_*$  and TKE favor the accumulation of pollutants near the surface. In the case of decoupling, it is hard to generate turbulence through the interaction between the atmosphere and the surface. To detect the main sources of turbulence, Fig. 87 presents the height–time cross-section of horizontal wind speed under 2,000 m. The lowest height range of WPR is at 200 m below which observations are seriously interfered by the hard-target returns of around buildings or trees. From Fig. 87a, strong wind occurs at night of 26 November 2016 with maximal wind speed larger than  $15 \text{ m s}^{-1}$ . For Case-2, there is also strong wind happening in the ABL right before the transitions between the CS and TS (Fig. 87b). After detecting the horizontal wind field, we found that the strong wind in the ABL is generally associated with the happening of LLJs. Fig. 98 takes three profiles as examples to illustrate the LLJ in the ABL. The vertical ‘nose’ shape of LLJs provides wind shear at upper levels, working as an elevated source of turbulent mixing. Then this turbulence is transported downward to the surface, resulting in non-stationary increase of turbulent mixing at lower levels. The differences in phase and strength of intermittency at three levels in Fig. 6 indicate that the wind shear associated with the LLJ ‘nose’ may play an important part in the generation and transport of turbulence in the ABL. Previous study (Wei et al., 2014) has revealed that the LLJ is a common phenomenon in Tianjin region, due to the combined effects of plain terrain for inertial oscillation (Lundquist, 2003) and strong baroclinicity related to the land–sea temperature contrast offshore (Parish, 2000). In addition, the reduced convection in winter is helpful to maintain the LLJs even during the daytime. In a word, the frequent LLJs in Tianjin region may be a key factor to understand the mechanisms of intermittent turbulence.

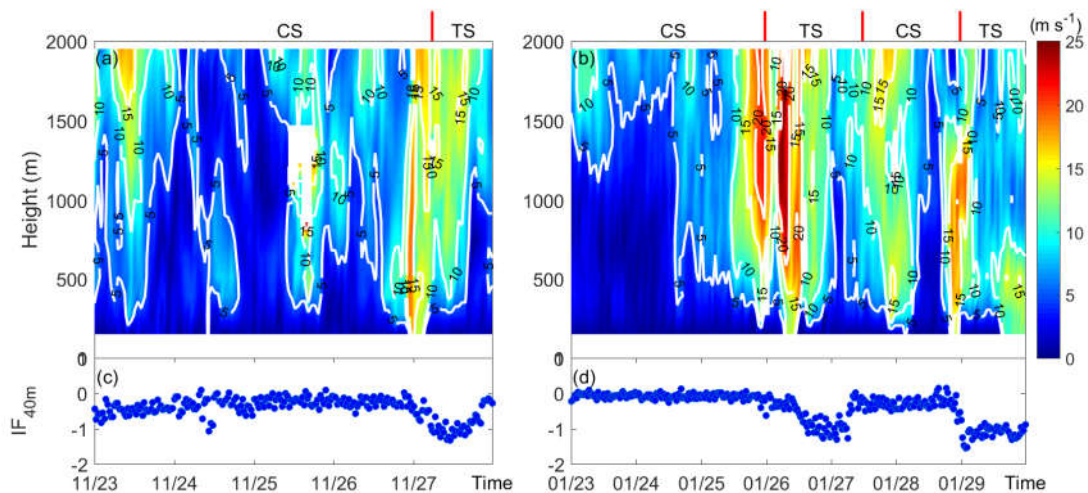
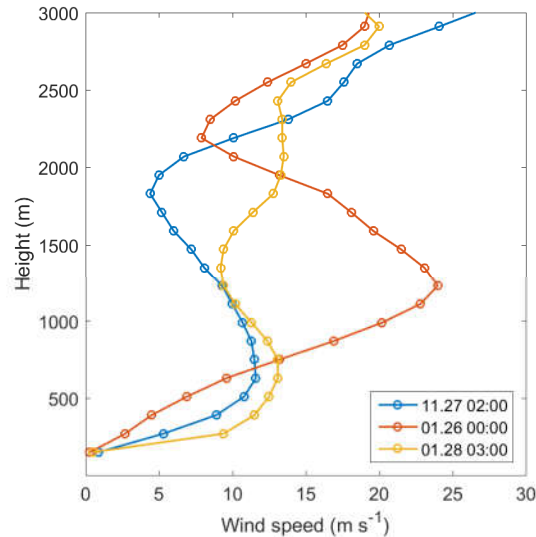


Figure 87. Height–time cross-section of horizontal wind speed observed by WPR for (a) Case-1 and (b) Case-2. (c) – (d) present the corresponding IF at 40 m.



5 Figure 89. Sample LLJ profiles for three transitions between CSs and TSs.

Finally, we ~~summary-summarize~~ the mechanism of intermittent turbulence affecting the  $PM_{2.5}$  concentration near the surface in a schematic figure in Fig. 109. In the beginning, the inversion layer near the surface enhances due to some favorable conditions including steady synoptic systems, stagnant wind, high temperature and high RH, which leads to the gradual accumulation of particles in the lower boundary layer. Such a process is named as the cumulative stage or CS, during which the turbulence near the surface is too weak to transport pollutants upward. In this case, if there existed LLJs (or other motions) in the ABL, the turbulence could be generated by the strong wind shear associated with the LLJs and then transport downward, resulting in intermittent turbulence at lower levels. The suddenly increased vertical mixing is helpful for the abrupt dissipation of  $PM_{2.5}$  near the surface.

15

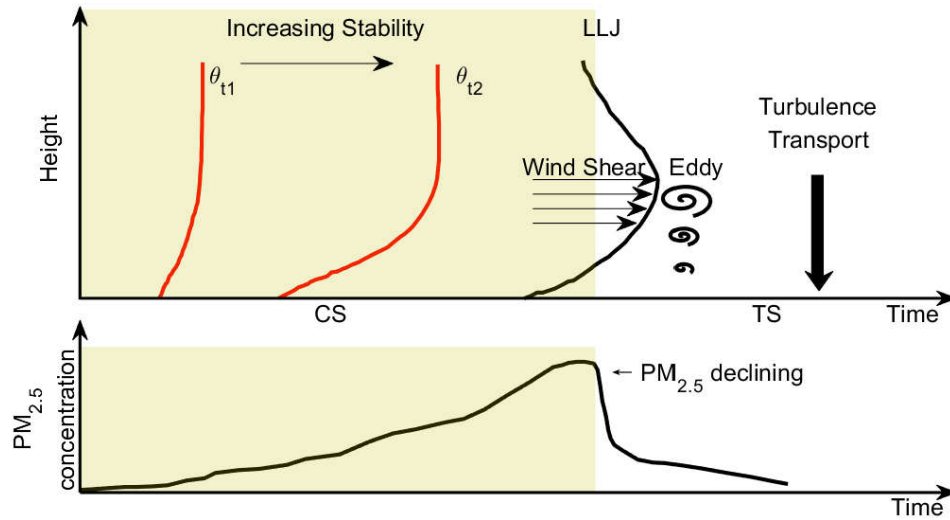


Figure 910. Schematic of how intermittent turbulence affects the dissipation of PM<sub>2.5</sub> near the surface.

#### 4 Conclusion

5 In the winter of 2016–2017, severe air pollution events haunted the North China Plain. Extremely high concentration of PM<sub>2.5</sub> threatens the health of the large population living in this region. In this work, two cases in Tianjin (39.00°N, 117.43°E), China were drawn upon to study the effects of intermittent turbulence on the improvement of air quality near the surface. Observations from a 255-m tower, a CFL-03 WPR and a TEOM 1405-DF system were analyzed to investigate the features of boundary-layer structure and PM<sub>2.5</sub> concentration. In order to measure the levels of turbulent intermittency, an index, called intermittent factor (IF), was proposed based on the arbitrary-order HSA which is more suitable for the analyses of nonlinear and non-stationary signals.

At first, due to the absorbed solar radiation by upper air pollutants and the reduced loss of surface longwave outgoing radiation, the inversion layer enhances with stronger heating of upper air layers. The stability function  $z/L$  keeps at high values ( $\gg 1$ ) at night and the stagnant wind field impedes the transport of pollutants. Additionally, high RH and steady cyclone system further aggravate the air pollution. All these factors result in the accumulation of pollutants near the surface.

15 On the other hand, the concentration of PM<sub>2.5</sub> undergoes rapid decrease during the dissipation periods, dropping from more than  $250 \mu\text{g m}^{-3}$  to less than  $50 \mu\text{g m}^{-3}$  within a few hours. The dispersion of pollutants coincides with the enhanced turbulent mixing in the ABL. The mean values of  $u_*$  and TKE rise to 2–9 times those of the polluted periods. The Hilbert-based exponent scaling function  $\xi(q)$  shows great deviations from K41's theoretical result of  $q/3$  by a set of concave curves, indicating that the enhanced turbulence in the ABL when entering the TS is intermittent rather than continuous or fully

developed. Using the IF index derived from the vertical wind speed, the abrupt change in IF at 40 m is in agreement with the sharp drop of PM<sub>2.5</sub> concentration. In addition, the occurrence and strength of intermittent turbulence differ with observation levels. In short, the higher the level is, the earlier the turbulence happens and the stronger the intermittency is, which implies that turbulence is mainly generated at upper levels and then transported to the surface. For 40 m, a cut-off value of IF (-0.50) indicates the initiation of strong turbulent intermittency in the ABL, while this is not a universal value and the threshold varies with different cases.

From the observation of WPR, LLJs were detected right before the dispersion of PM<sub>2.5</sub>. Previous work (Marht, 2014) has pointed out that the stronger wind shear at the height of LLJ ‘nose’ can be a source of turbulence under the condition of decoupling between the atmosphere and the surface. In this work, LLJs play a key role in the generation of upper-level turbulence. The subsequent downward transport of turbulence leads to intermittent mixing near the surface, thus enhancing the vertical dispersion of PM<sub>2.5</sub> and improving the air quality.

*Data availability.* Data used in this study are available from the corresponding author upon request (hsdq@pku.edu.cn).

*Competing interests.* The authors declare that they have no conflict of interest.

*Acknowledgement.* This work was jointly funded by grant from National Key R&D Program of China (2016YFC0203300), the National Natural Science Foundation of China (91544216, 41705003, 41475007, 41675018). We also thank Dr. Gao Shanhong at Ocean University of China for providing historical weather-condition charts. Many thanks to Sr. Engr. Yao Qing and Liu Jinle at Tianjin Municipal Meteorological Bureau for their help with the data observation.

## References

Anfossi, D., Oetl, D., Degrazia, G. and Goulart, A.: An analysis of sonic anemometer observations in low wind speed conditions, *Boundary-Layer Meteorol.*, 114(1), 179–203, doi:10.1007/s10546-004-1984-4, 2005.

[Banta, R. M., Mahrt, L., Vickers, D., Sun, J., Balsley, B. B., Pichugina, Y. L. and Williams, E. J.: The very stable boundary layer on nights with weak low-level jets, \*J. Atmos. Sci.\*, 64\(9\), 3068-3090, doi: 10.1175/jas4002.1, 2007.](#)

Banta, R. M., Pichugina, Y. L. and Brewer, W. A.: Turbulent Velocity-Variance Profiles in the Stable Boundary Layer Generated by a Nocturnal Low-Level Jet, *J. Atmos. Sci.*, 63(11), 2700–2719, doi:10.1175/JAS3776.1, 2006.

[Banta, R. M., Pichugina, Y. L. and Newsom, R. K.: Relationship between low-level jet properties and turbulence kinetic energy in the nocturnal stable boundary layer, \*J. Atmos. Sci.\*, 60\(20\), 2549-2555, doi: 10.1175/1520-0469\(2003\)060<2549:rbljpa>2.0.co;2, 2003.](#)

- Basu, S., Fofoula-Georgiou, E. and Porté-Agel, F.: Synthetic turbulence, fractal interpolation, and large-eddy simulation, *Phys. Rev. E*, 70(2), 26310, doi:10.1103/PhysRevE.70.026310, 2004.
- Bressi, M., Sciare, J., Gherzi, V., Bonnaire, N., Nicolas, J. B., Petit, J. E., Moukhtar, S., Rosso, A., Mihalopoulos, N. and Féron, A.: A one-year comprehensive chemical characterisation of fine aerosol (PM<sub>2.5</sub>) at urban, suburban and rural background sites in the region of Paris (France), *Atmos. Chem. Phys.*, 13(15), 7825–7844, doi:10.5194/acp-13-7825-2013, 2013.
- [Chan, C. K. and Yao, X.: Air pollution in mega cities in China, \*Atmos. Environ.\*, 42, 1–42, doi: 10.1016/j.atmosenv.2007.09.003, 2008.](https://doi.org/10.1016/j.atmosenv.2007.09.003)
- Cohen, L.: Time-frequency analysis, Prentice Hall, Englewood Cliffs, NJ, 1995.
- Derbyshire, S. H.: Boundary-layer decoupling over cold surfaces as a physical boundary-instability, *Boundary-Layer Meteorol.*, 90(2), 297–325, doi:10.1023/A:1001710014316, 1999.
- Dominici, F., Greenstone, M. and Sunstein, C. R.: Particulate Matter Matters, *Science*, 344(6181), 257–259, doi: 10.1126/science.1247348, 2014.
- Engelhart, G. J., Hildebrandt, L., Kostenidou, E., Mihalopoulos, N., Donahue, N. M. and Pandis, S. N.: Water content of aged aerosol, *Atmos. Chem. Phys.*, 11(3), 911–920, doi:10.5194/acp-11-911-2011, 2011.
- Faust, J. A., Wong, J. P. S., Lee, A. K. Y., and Abbatt, J. P.: Role of Aerosol Liquid Water in Secondary Organic Aerosol Formation from Volatile Organic Compounds, *Environ. Sci. Technol.*, 51(3): 1405-1413, doi: 10.1021/acs.est.6b04700, 2017.
- Frisch, U.: Fully developed turbulence and intermittency, *Ann. NY. Acad. Sci.*, 357(1): 359-367, doi: 10.1111/j.1749-6632.1980.tb29703.x, 1980.
- Frisch, U.: Turbulence: the legacy of AN Kolmogorov, Cambridge university press, Great Britain, 1995.
- Gao, S., Wang, Y., Huang, Y., Zhou, Q., Lu, Z., Shi, X. and Liu, Y.: Spatial statistics of atmospheric particulate matter in China, *Atmos. Environ.*, 134, 162–167, doi:10.1016/j.atmosenv.2016.03.052, 2016.
- [Ha, K. J., Hyun, Y. K., Oh, H. M., Kim, K. E. and Mahrt, L.: Evaluation of boundary layer similarity theory for stable conditions in CASES-99, \*Mon. Weather Rev.\*, 135\(10\), 3474-3483, doi: 10.1007/bf00119423, 2007.](https://doi.org/10.1007/bf00119423)
- Helgason, W. and Pomeroy, J. W.: Characteristics of the near-surface boundary layer within a mountain valley during winter, *J. Appl. Meteorol. Climatol.*, 51(3), 583–597, doi:10.1175/JAMC-D-11-058.1, 2012.
- Holtslag, A. A. M.: BOUNDARY LAYER (ATMOSPHERIC) AND AIR POLLUTION | Modeling and Parameterization, in *Encyclopedia of Atmospheric Sciences*, vol. 1, pp. 265–273, Elsevier., 2015.
- Huang, N., Shen, Z., Long, S., Wu, M., Shih, H., Zheng, Q., Yen, N., Tung, C. and Liu, H.: The empirical mode decomposition and the Hilbert spectrum for nonlinear and non-stationary time series analysis, *Proc. R. Soc. A Math. Phys. Eng. Sci.*, 454(1971), 903–995, doi:10.1098/rspa.1998.0193, 1998.
- Huang, N. E., Shen, Z. and Long, S. R.: A new view of nonlinear water waves: the Hilbert Spectrum, *Annu. Rev. Fluid Mech.*, 31(1), 417–457, doi:10.1146/annurev.fluid.31.1.417, 1999.

- Huang, Y., Schmitt, F. G., Lu, Z. and Liu, Y.: Analysis of daily river flow fluctuations using empirical mode decomposition and arbitrary order Hilbert spectral analysis, *J. Hydrol.*, 373(1–2), 103–111, doi:10.1016/j.jhydrol.2009.04.015, 2009.
- Huang, Y. X., Schmitt, F. G., Lu, Z. M. and Liu, Y. L.: An amplitude-frequency study of turbulent scaling intermittency using Empirical Mode Decomposition and Hilbert Spectral Analysis, *EPL (Europhysics Lett.)*, 84(4), 40010, doi:10.1209/0295-5075/84/40010, 2008.
- Huang, Y. X., Schmitt, F. G., Hermand, J. P., Gagne, Y., Lu, Z. M. and Liu, Y. L.: Arbitrary-order Hilbert spectral analysis for time series possessing scaling statistics: Comparison study with detrended fluctuation analysis and wavelet leaders, *Phys. Rev. E*, 84(1), 16208, doi:10.1103/PhysRevE.84.016208, 2011.
- Jiang, C., Wang, H., Zhao, T., Li, T., and Che, H.: Modeling study of PM 2.5 pollutant transport across cities in China's Jing-Jin-Ji region during a severe haze episode in December 2013, *Atmos. Chem. Phys.*, 15(10), 5803-5814, doi: 10.5194/acpd-15-3745-2015, 2015
- Klipp, C. L. and Mahrt, L.: Flux-gradient relationship, self-correlation and intermittency in the stable boundary layer, *Q. J. R. Meteorol. Soc.*, 130(601), 2087–2103, doi:10.1256/qj.03.161, 2004.
- Lundquist, J. K.: Intermittent and Elliptical Inertial Oscillations in the Atmospheric Boundary Layer, *J. Atmos. Sci.*, 60(1997), 2661–2673, doi:10.1175/1520-0469(2003)060<2661:IAEIOI>2.0.CO;2, 2003.
- Mahrt, L.: Nocturnal Boundary-Layer Regimes, *Boundary-layer Meteorol.*, 88(2), 255–278, doi:10.1023/A:1001171313493, 1998.
- Mahrt, L.: Stratified Atmospheric Boundary Layers, *Boundary-Layer Meteorol.*, 90(3), 375–396, doi:10.1023/A:1001765727956, 1999.
- Mahrt, L.: Stably Stratified Atmospheric Boundary Layers, *Annu. Rev. Fluid Mech.*, 46, 23–45, doi:10.1146/annurev-fluid-010313-141354, 2014.
- Miao, Y., Guo, J., Liu, S., Liu, H., Zhang, G., Yan, Y. and He, J.: Relay transport of aerosols to Beijing-Tianjin-Hebei region by multi-scale atmospheric circulations, *Atmos. Environ.*, 165, 35–45, doi:10.1016/j.atmosenv.2017.06.032, 2017.
- Nel, A.: ATMOSPHERE: Enhanced: Air Pollution-Related Illness: Effects of Particles, *Science*, 308(5723), 804–806, doi:10.1126/science.1108752, 2005.
- Noone, D., Risi, C., Bailey, A., Berkelhammer, M., Brown, D. P., Buenning, N., Gregory, S., Nusbaumer, J., Schneider, D., Sykes, J., Vanderwende, B., Wong, J., Meillier, Y. and Wolfe, D.: Determining water sources in the boundary layer from tall tower profiles of water vapor and surface water isotope ratios after a snowstorm in Colorado, *Atmos. Chem. Phys.*, 13(3), 1607–1623, doi:10.5194/acp-13-1607-2013, 2013.
- Parish, T. R.: Forcing of the Summertime Low-Level Jet along the California Coast, *J. Appl. Meteorol.*, 39(12), 2421–2433, doi:10.1175/1520-0450(2000)039<2421:FOTSLL>2.0.CO;2, 2000.
- Petäjä, T., Järvi, L., Kerminen, V. M., Ding, A. J., Sun, J. N., Nie, W., Kujansuu, J., Virkkula, A., Yang, X., Fu, C. B., Zilitinkevich, S. and Kulmala, M.: Enhanced air pollution via aerosol-boundary layer feedback in China, *Sci. Rep.*, 6(January), doi:10.1038/srep18998, 2016.



- Petters, M. D. and Kreidenweis, S. M.: A single parameter representation of hygroscopic growth and cloud condensation nucleus activity &ndash; Part 2: Including solubility, *Atmos. Chem. Phys. Discuss.*, 8(2), 5939–5955, doi:10.5194/acpd-8-5939-2008, 2008.
- Poulos, G. S., Blumen, W., Fritts, D. C., Lundquist, J. K., Sun, J., Burns, S. P., Nappo, C., Banta, R., Newsom, R., Cuxart, J., Terradellas, E., Balsley, B. and Jensen, M.: CASES-99: A comprehensive investigation of the stable nocturnal boundary layer, *Bull. Am. Meteorol. Soc.*, 83(4), 555–581, doi:10.1175/1520-0477(2002)083<0555:CACIOT>2.3.CO;2, 2002.
- Quan, J., Liu, Q., Li, X., Gao, Y., Jia, X., Sheng, J. and Liu, Y.: Effect of heterogeneous aqueous reactions on the secondary formation of inorganic aerosols during haze events, *Atmos. Environ.*, 122, 306–312, doi:10.1016/j.atmosenv.2015.09.068, 2015.
- 10 Ren, Y., Zheng, S., Wei, W., Wu, B., Zhang, H., Cai, X. and Song, Y.: Characteristics of the Turbulent Transfer during the Heavy Haze in Winter 2016 / 17 in Beijing, *J. Meteorol. Res.*, doi:10.1007/s13351-018-7072-3, 2017.
- Salmond, J. A.: Wavelet analysis of intermittent turbulence in a very stable nocturnal boundary layer: implications for the vertical mixing of ozone, *Boundary-Layer Meteorol.*, 114(3), 463–488, doi:10.1007/s10546-004-2422-3, 2005.
- Schmitt, F. G., Huang, Y., Lu, Z., Liu, Y. and Fernandez, N.: Analysis of velocity fluctuations and their intermittency properties in the surf zone using empirical mode decomposition, *J. Mar. Syst.*, 77(4), 473–481, doi:10.1016/j.jmarsys.2008.11.012, 2009.
- 15 Shen, Z., Cui, G. and Zhang, Z.: Turbulent dispersion of pollutants in urban-type canopies under stable stratification conditions, *Atmos. Environ.*, 156, 1–14, doi:10.1016/j.atmosenv.2017.02.017, 2017.
- Smedman, A. S., Bergström, H. and Högström, U.: Spectra, variances and length scales in a marine stable boundary layer dominated by a low level jet, *Boundary-Layer Meteorol.*, 76(3), 211–232, doi:10.1007/BF00709352, 1995.
- 20 Sorbjan, Z. and Czerwinska, A.: Statistics of Turbulence in the Stable Boundary Layer Affected by Gravity Waves, *Boundary-Layer Meteorol.*, 148(1), 73–91, doi:10.1007/s10546-013-9809-y, 2013.
- Strang, E. J. and Fernando, H. J. S.: Entrainment and mixing in stratified shear flows, *J. Fluid Mech.*, 428(6S), 349–386, doi:10.1017/S0022112000002706, 2001.
- 25 Stull, R.B.: *An Introduction to Boundary Layer Meteorology*, Kluwer Academic, USA, 1988.
- Sun, J., Mahrt, L., Nappo, C. and Lenschow, D. H.: Wind and Temperature Oscillations Generated by Wave–Turbulence Interactions in the Stably Stratified Boundary Layer, *J. Atmos. Sci.*, 72(4), 1484–1503, doi:10.1175/JAS-D-14-0129.1, 2015.
- Sun, Y., Zhuang, G., Wang, Y., Han, L., Guo, J., Dan, M., Zhang, W., Wang, Z. and Hao, Z.: The air-borne particulate pollution in Beijing - Concentration, composition, distribution and sources, *Atmos. Environ.*, 38(35), 5991–6004, doi:10.1016/j.atmosenv.2004.07.009, 2004.
- 30 Tang, G., Zhang, J., Zhu, X., Song, T., Münkkel, C., Hu, B., Schäfer, K., Liu, Z., Zhang, J., Wang, L., Xin, J., Suppan, P. and Wang, Y.: Mixing layer height and its implications for air pollution over Beijing, China, *Atmos. Chem. Phys.*, 16(4), 2459–2475, doi:10.5194/acp-16-2459-2016, 2016.

- Terradellas, E., Soler, M. R., Ferreres, E. and Bravo, M.: Analysis of oscillations in the stable atmospheric boundary layer using wavelet methods, *Boundary-Layer Meteorol.*, 114, 489–518, doi:10.1007/s10546-004-1293-y, 2005.
- Thompson, T. M., Saari, R. K. and Selin, N. E.: Air quality resolution for health impact assessment: Influence of regional characteristics, *Atmos. Chem. Phys.*, 14(2), 969–978, doi:10.5194/acp-14-969-2014, 2014.
- 5 [Vindel, J. M., Yagüe, C. and Redondo, J. M.: Structure function analysis and intermittency in the atmospheric boundary layer, \*Nonlinear. Proc. Geoph.\*, 15\(6\), 915-929, doi: 10.5194/npg-15-915-2008, 2008.](#)
- Vindel, J. M. and Yagüe, C.: Intermittency of Turbulence in the Atmospheric Boundary Layer: Scaling Exponents and Stratification Influence, *Boundary-Layer Meteorol.*, 140(1), 73–85, doi:10.1007/s10546-011-9597-1, 2011.
- Wang, T., Nie, W., Gao, J., Xue, L. K., Gao, X. M., Wang, X. F., Qiu, J., Poon, C. N., Meinardi, S., Blake, D., Wang, S. L.,
- 10 Ding, A. J., Chai, F. H., Zhang, Q. Z. and Wang, W. X.: Air quality during the 2008 Beijing Olympics: Secondary pollutants and regional impact, *Atmos. Chem. Phys.*, 10(16), 7603–7615, doi:10.5194/acp-10-7603-2010, 2010.
- Wang, X., Wang, W., Yang, L., Gao, X., Nie, W., Yu, Y., Xu, P., Zhou, Y. and Wang, Z.: The secondary formation of inorganic aerosols in the droplet mode through heterogeneous aqueous reactions under haze conditions, *Atmos. Environ.*, 63, 68–76, doi:10.1016/j.atmosenv.2012.09.029, 2012.
- 15 Wang, X., Dickinson, R. E., Su, L., Zhou, C. and Wang, K.: PM 2.5 Pollution in China and How It Has Been Exacerbated by Terrain and Meteorological Conditions, *Bull. Am. Meteorol. Soc.*, doi:10.1175/BAMS-D-16-0301.1, 2017.
- Wei, W., Zhang, H. S. and Ye, X. X.: Comparison of low-level jets along the north coast of China in summer, *J. Geophys. Res. Atmos.*, 119(16), 9692–9706, doi:10.1002/2014JD021476, 2014.
- Wei, W., Schmitt, F. G., Huang, Y. X. and Zhang, H. S.: The Analyses of Turbulence Characteristics in the Atmospheric
- 20 Surface Layer Using Arbitrary-Order Hilbert Spectra, *Boundary-Layer Meteorol.*, 159(2), 391–406, doi:10.1007/s10546-015-0122-9, 2016.
- Wei, W., Wang, M., Zhang, H., He, Q., Ali, M. and Wang, Y.: Diurnal characteristics of turbulent intermittency in the Taklimakan Desert, *Meteorol. Atmos. Phys.*, doi:10.1007/s00703-017-0572-3, 2017.
- Van de Wiel, B. J. H., Moene, a. F., Hartogensis, O. K., De Bruin, H. a. R. and Holtslag, a. a. M.: Intermittent Turbulence
- 25 in the Stable Boundary Layer over Land. Part III: A Classification for Observations during CASES-99, *J. Atmos. Sci.*, 60(20), 2509–2522, doi:10.1175/1520-0469(2003)060<2509:ITITSB>2.0.CO;2, 2003.
- Van de Wiel, B. J. H., Moene, A. F., Jonker, H. J. J., Baas, P., Basu, S., Donda, J. M. M., Sun, J. and Holtslag, A. A. M.: The Minimum Wind Speed for Sustainable Turbulence in the Nocturnal Boundary Layer, *J. Atmos. Sci.*, 69(11), 3116–3127, doi:10.1175/JAS-D-12-0107.1, 2012.
- 30 Ye, X., Wu, B. and Zhang, H.: The turbulent structure and transport in fog layers observed over the Tianjin area, *Atmos. Res.*, 153, 217–234, doi:10.1016/j.atmosres.2014.08.003, 2014.
- Ye, X., Song, Y., Cai, X. and Zhang, H.: Study on the synoptic flow patterns and boundary layer process of the severe haze events over the North China Plain in January 2013, *Atmos. Environ.*, 124(January 2013), 129–145, doi:10.1016/j.atmosenv.2015.06.011, 2016.

- Yin, Z. and Wang, H.: Role of atmospheric circulations in haze pollution in December 2016, *Atmos. Chem. Phys.*, 17(18), 11673–11681, doi:10.5194/acp-17-11673-2017, 2017.
- Yin, Z., Wang, H. and Chen, H.: Understanding severe winter haze events in the North China Plain in 2014: Roles of climate anomalies, *Atmos. Chem. Phys.*, 17(3), 1641–1651, doi:10.5194/acp-17-1641-2017, 2017.
- 5 Zhang, H., Chen, J. and Park, S.: Turbulence structure in unstable conditions over various surfaces, *Boundary-Layer Meteorol.*, 100(2), 243–261, doi:10.1023/A:1019223316895, 2001.
- Zhang, H., Wang, S., Hao, J., Wang, X., Wang, S., Chai, F. and Li, M.: Air pollution and control action in Beijing, *J. Clean. Prod.*, 112, 1519–1527, doi:10.1016/j.jclepro.2015.04.092, 2016.
- Zhang, J. P., Zhu, T., Zhang, Q. H., Li, C. C., Shu, H. L., Ying, Y., Dai, Z. P., Wang, X., Liu, X. Y., Liang, A. M., Shen, H.
- 10 X. and Yi, B. Q.: The impact of circulation patterns on regional transport pathways and air quality over Beijing and its surroundings, *Atmos. Chem. Phys.*, 12(11), 5031–5053, doi:10.5194/acp-12-5031-2012, 2012.
- Zhang, Y.-L. and Cao, F.: Fine particulate matter (PM<sub>2.5</sub>) in China at a city level, *Sci. Rep.*, 5(October), 14884, doi:10.1038/srep14884, 2015.
- [Zhang, Y., Zhu, B., Gao, J., Kang, H., Yang, P., Wang, L., and Zhang, J.: The source apportionment of primary PM<sub>2.5</sub> in an aerosol pollution event over Beijing-Tianjin-Hebei region using WRF-Chem, \*China, Aerosol Air Qual. Res.\*, 17, 2966-2980, doi: 10.4209/aaqr.2016.10.0442, 2017.](#)
- 15 [Zheng, G. J., Duan, F. K., Su, H., Ma, Y. L., Cheng, Y., Zheng, B., Zhang, Q., Huang, T., Kimoto, T., Chang, D., Pöschl, U., Cheng, Y. F. and He, K. B.: Exploring the severe winter haze in Beijing: The impact of synoptic weather, regional transport and heterogeneous reactions, \*Atmos. Chem. Phys.\*, 15\(6\), 2969–2983, doi:10.5194/acp-15-2969-2015, 2015a.](#)
- 20 Zheng, S., Pozzer, A., Cao, C. X. and Lelieveld, J.: Long-term (2001-2012) concentrations of fine particulate matter (PM<sub>2.5</sub>) and the impact on human health in Beijing, China, *Atmos. Chem. Phys.*, 15(10), 5715–5725, doi:10.5194/acp-15-5715-2015, 2015b.
- [Zheng, B., Zhang, Q., Zhang, Y., He, K. B., Wang, K., Zheng, G. J., Duan, F. K., Ma, Y. L., and Kimoto, T.: Heterogeneous chemistry: a mechanism missing in current models to explain secondary inorganic aerosol formation during the January 2013 haze episode in North China, \*Atmos. Chem. Phys.\*, 15, 2031–2049, doi:10.5194/acp-15-2031-2015, 2015c.](#)
- 25 Zhong, J., Zhang, X., Wang, Y., Sun, J., Zhang, Y., Wang, J., Tan, K., Shen, X., Che, H., Zhang, L., Zhang, Z., Qi, X., Zhao, H., Ren, S. and Li, Y.: Relative contributions of boundary-layer meteorological factors to the explosive growth of PM<sub>2.5</sub> during the red-alert heavy pollution episodes in Beijing in December 2016, *J. Meteorol. Res.*, 31(5), 809–819, doi:10.1007/s13351-017-7088-0, 2017.